Herbert Merkle

Innovation-Report:
Development of Soiling Process Characterisation Methods for Solar Mirrors, for analysing Mirror Cleaning Processes

(Submission six)

School of Aerospace, Transport and Manufacturing
EngD Sustainability, Manufacturing and Sustainable Materials

Engineering Doctorate
Academic Year: 2019-2023

Supervisor: Dr. Peter King (University Cranfield),
Prof. Christopher Sansom (University of Derby)
Associate Supervisor: Dr. Tara Schiller (University of Warwick)

September 2023

School of Aerospace, Transport and Manufacturing
EngD Sustainability, Manufacturing and sustainable Materials

Engineering Doctorate

Academic Year 2019-2023

Herbert Merkle

Innovation–Report: Development of Soiling Process Characterisation Methods for Solar Mirrors, for analysing Mirror Cleaning Processes

(Submission six)

Supervisor: Dr. Peter King (Cranfield University),
Prof. Christopher Sansom (University of Derby),
Associate Supervisor: Dr. Tara Schiller (University of Warwick)

September 2023

This thesis is submitted in partial fulfilment of the requirements for the degree of Engineering Doctorate

Academic Integrity Declaration

I declare that:

- the thesis submitted has been written by me alone.
- the thesis submitted has not been previously submitted to this university or any other.
- that all content, including primary and/or secondary data, is true to the best of my knowledge.
- that all quotations and references have been duly acknowledged according to the requirements of academic research.

I understand that to knowingly submit work in violation of the above statement will be considered by examiners as academic misconduct.

Abstract

Concentrated Solar Power has the potential to provide power for the developing global economies towards a sustainable future. This solar radiation-based technology, reflects the radiation received by a solar mirror onto a receiver device which absorbs heat. Maintenance is required to keep the solar mirrors clean, and remove airborne particulate matter that settles on the mirror, which has an impact on the solar collector efficiency. Constant research to optimize cleaning methods and cleaning–strategies is paramount.

An artificial soiling test rig and soiling methods were developed, which are capable of simulating repeatable soiling events and to specific soiling load. These features are necessary to simulate cleaning cycles with a period of several days. The developed test rig has a capability to provide a minimum soiling load of 0.25g/m^2 and has a constant error of 16%. Repeatable soiling tests were carried out up to 10 times.

Extensive soiling experiments with two soiling materials (silt material and ground taken material from Almeria, Spain) and numerical simulation have revealed the exponential nature of the soiling process. An empirical model was formulated, which calculates specular reflectance, and includes material intrinsic parameters and soiling load data. This model highlighted the fact that compared to a linear model, between 7-20% lower soiling load is predicted, which potentially has a positive influence on cleaning cycles and therefore the costs attributed to them.

A simulation series of a 10day cleaning cycles, which includes repeatable soiling and condensation events, used the artificial soiling test rig and a cooling plate located in a dry chamber. The adhesion effect (particle caking and capillary aging) were analysed by a centrifuge and the coverage ratio of the mirror samples before and after the experiments were calculated. It was noted that the repeatable soiling test (soiling and condensation) had a visible difference compared to the one-off soiling and condensation test series.

The experimental modelling work will help to improve the considerable maintenance effort involved in mirror cleaning in solar field operations.

Keywords:

Concentrated Solar Power, soiling process characterisation, artificial soiling test rig, soiling load reflectance model, adhesion effect, centrifuge test, condensation

Acknowledgements

It is my pleasure to express my deepest appreciation to all the individuals who help and supported me during the last four years.

In particular to my mentors Prof. Christopher Sansom and Dr. Peter King, who encouraged me throughout my journey in progressing my studies. It was always a delight to discuss new ideas and approaches when needed.

Furthermore, I am deeply indebted to my supervisor and friend Dr. Tara Schiller from University of Warwick, for her never ending help and support during- and in particular in the last phase of the project. Without you I never would be able to finalize this project.

The author would like to thank to Mr Mary McGovern and ADTEC Plasma Technology & ADTEC Europe for providing financial and technical support and also to Adam Bennet who provided advice in difficult times.

Also, I would like to thank to Cranfield University for the facilities and equipment needed to progress my studies and all stuff members of the Cranfield University in particular Mr. Collins, for his advice throughout the years in the lab.

I also would like to acknowledge my fellow researcher, who help enormously when things did not work, in particular Koldo, Michael, Heather Almond, and Mounia Karim.

And finally, I am deeply grateful to my family, my wife Malgorzata and son Oliver who certainly haven't always had a good time with me. Thanks for the help and support, without you I would not have finished my work at Cranfield University.

This project is funded by the UK EPSRC under grants EP/K503241/1 and EP/L016389/1.

Table of Contents

List of Figures

List of Tables

List of Equations

Nomenclature

Optical efficiency	(η_{opt})	[1]
Capture fraction	(Γ)	[1]
Reflectance of reflector surfaces	(ρ)	[1]
Transmittance of any glass/plastic cover or windows	(τ)	[1]
Absorbance of absorber/receiver surface	(α)	[1]
Total degradation cost	(L_{tot})	[1]
Reflectance of clean reflector	(ρ_0)	[1]
Reflectance of current reflector	(ρ_t)	[1]
Current electricity price	(p)	[1]
Direct Normal Irradiance	(DNI)	[1]
Total reflector efficiency	(η)	[1]
Cleaning cost (per $1m^2$)	(C_{cl})	[1]
Control factor cleaning cost (per $1m^2$)	(A_k)	[1,0]
Time:	(t)	s
Mass Deposition Density:	(MDD)	g/m^2
Mass soiled:	(m_{soil})	kg
Area soiled:	(a_{soil})	m^2
Coverage ratio geometric:	(q)	[1]
Area covered:	(a_{cover})	m^2
geometric: geo		
effective: eff		
Mass deposition density of the simulated particles:	$(MDD_{(n_{part}^{NORM})})$	g/m^2
Mass of deposite particles:	(m_{part}^{soiled})	g
Total simulated soiling area:	$(a_{part}^{soiling})$	m^2
Number of area elements:	$(N_{a\text{-}el})$	[1]

Normalized number of particles:	$\left(n_{part}^{NORM}\right)$	[1]
Soiling coefficient:	(C_{MDD})	g/m^2
Constant (geometric):	$\left(c_{geo}^{OPT}\right)$	0.9423[1]
Constant (effective):	$\left(c_{eff}^{OPT}\right)$	0.4705[1]
Mean solar weighted specular reflectance:	(RSe)	[1]
Particle diameter (De Brouckere):	($D_{[4,3]}$)	μm
Particle density:	(ρ_{part})	kg/m^3
Test sequences for mass and density measurements	(sequ)	[1]
Coefficients for power-function:	(a, b)	[1]
Variable	(p)	[1]
Relative Humidity:	(rH)	%
Velocity:	(V)	m/s
Particle radius	(r)	m
Mass:	(m)	kg
Gravitational force:	(F_{grav})	N
Lift force:	(F_{lift})	N
Centripetal force:	(F_{cent})	N
Drag force:	(F_{drag})	N
Adhesion force:	(F_{adh})	N
Detachment Force:	(F_{det})	N
Density air:	(ρ_{air})	1.184kg/m^3
Particle diameter (vertical projection):	(D_{part})	μm
Friction / shear velocity:	(u_{δ})	m/s
Kinematic viscosity air (300K):	(ν)	1.568x10^{-5}m^2/s
Concentration Factor:	(C_r)	[1]

List of Abbreviations

American Society for Testing and Materials	ASTM
Centro de Investigaciones Energéticas, Medioambientales y Tecnológicas	CIEMAT
Concentrated Solar Power	CSP
Deutsches Institute fuer Normung	DIN
Deutsches Zentrum für Luft-und Raumfahrt	DLR
Health and Safety Executive	HSE
Plataforma Solar de Almeria	PSA
International System Organisation	ISO
Total (global) Final Consumption	TFC
Work Package	WP

1 Introduction

The Innovation–Report presents a summary of the research work carried out, necessary for this thesis. The development of experimental methods relevant for soiling process are on the focus and therefore represent the main outcome. Furthermore, the exploitation of developed methods are also conducted.

The research project was divided into main sections according to the submissions documents. The individual submissions provide an in depth view of the development throughout the project, the first “try out” results of the experimental work. The majority of the work was conducted at Cranfield University, however the University of Warwick provided additional support with the experimental work. The international placement provided additional results and experiences, which adds to the overall outcome of this research project.

The Introduction provides an overview of the Innovation–Report, its structure, the project target, results, and the innovation aspect of the research results.

1.1 Research Motivation and Focus

This document highlights the development of experimental methods that focus on the soiling processes that interfere with the efficiency of the solar energy applications. In the age of climate change and global development of humans, it is obvious that more energy demand rather than less, is what civilisation is facing. Keeping this in mind, more problems will be created in the future originated by greenhouse gases if we carry on as before.

Renewable Energy source and in particular Concentrated Solar Power (CSP), provides an opportunity for the future to tackle this problem. However, due to particles in particular in desert like areas which are preferred locations for CSP applications, quickly reducing the efficiency of solar collectors in correlation to the soiling extent. This affects all solar collectors, solar thermal collector as well as photovoltaic collectors.

Improving the maintenance process, is the importance area in the solar energy industry and has to be further developed. Global research effort will be improved with the quality of experimental methods, which replicate the natural soiling process holistically in all the complexity of the soiling process. These aspects influence the final results, soiling load, particle adhesion and specular reflectance. Active cleaning operations (commercially) and self-cleaning process' (naturally from rainfall) are dependent on particle adhesion. In order to simulate particle adhesion, it is necessary to develop a method to provide accurate and reproducible artificially soiled mirror samples, which in turn implies the development of a test rig.

This research project was initiated by improving the cleaning process of solar mirrors by the use of atmospheric pressure plasma, sponsored by the company ADTEC Plasma Technology Co. Ltd London. The principle idea s to enhance the mirror surface to an extreme hydrophilic stage, which improves the condensation condition, which then improves the self–cleaning characteristic. This potentially extend the period between artificially-initiated cleaning cycles, i.e. those as a part of regular maintenance of the solar field. The original project was divided into two projects, one was focused on the characterisation process of soiled solar mirrors and the other on the soiling process in the context of CSP.

1.2 Aims and Objectives

The project is focused on providing an understanding of the fundamentals of the soiling process in solar applications, mainly in CSP. A literature review highlighted the complexity of the soiling process and finally the importance of particle adhesion. To replicate this complex of individual effects, which includes soiling load and condensation is a major target of this project. When possible, the developed methods, rigs and experiments will be used to exploit the opportunities provided, e.g. artificial soiling test rig.

Therefore, the project identified the following targets of development:

- Artificial soiling of mirror sample, which is repeatable and robust
- A method to replicate the soiling process in its complexity

1.3 Limitation of the Project

This project does not deal with the development of enhance plasma systems, suitable to clean or support the cleaning process of soiled solar mirrors.

The project is limited on CSP and therefore photovoltaic and vacuum tube collector are not part of this investigation, however the research results can be certainly be of value to these technologies. Only uncoated solar mirrors, as used in CSP are of interest in this research work. The self–cleaning effect and particle repelling coatings are not part of this project.

1.4 EngD Portfolio (Structure)

Eight submission were prepared including the Innovation–Report. Five submissions highlighted the project results and a further two submissions are the International Placement- and the Personnel Development-report. Figure 1 provides an overview of all submissions prepared.

1.4.1 Project–Motivation and Description (Submission one)

Submission one provides a comprehensive overview of the situation of solar energy as at present and the part which CSP plays in it. It highlights the importance of the solar mirror, and finally the importance of mitigation of soiling.

1.4.2 Methodology (Submission two)

Submission two presents an overview of the fundamental physics involved, the formulation of the aim and objectives and finally techniques' available and relevant for the project when appropriate. At this stage of the project, the student got in contact with the international research community in the area of interest (PSA and the international soiling group, Submission seven).

1.4.3 Artificial Soiling for Concentrated Solar Power Research (Submission three)

The first objective here was the development of an artificial soiling test-rig, including additional features other than those mentioned in literature, of which Submission three details. Repeating soiling, which mirrors the natural condition of soiling in real applications, is the main specification, and along with the sequential process also soiling to a specific soiling material mass is required. After the development stage, an extensive trail period followed which established the capability and limits of the artificial soiling test rig. The results were presented at the SolarPace 2021 Conference.

1.4.4 Basic Reflectance Model (Submission four)

Additional soiling experiments, measurements of the soiling load (mass deposition density and coverage ratio) and analysis followed. Submission four presents the first findings by creating and proving (simulation) an empirical model, which combines mass deposition density with coverage ratio, material property (size) and reflectance.

Figure 1 provides an overview of the Engineering Doctorate scheme's portfolio.

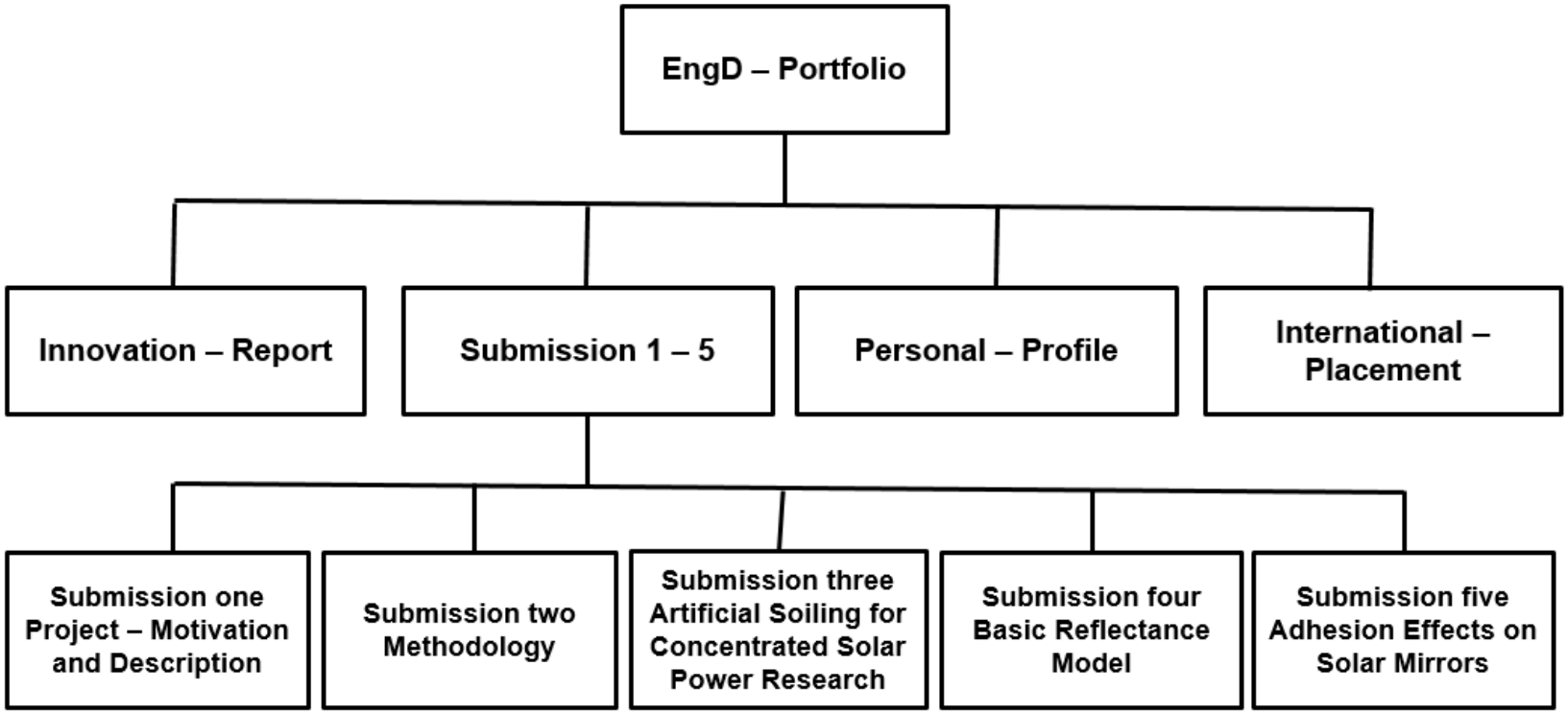

Fig. 1: Overview of the submissions for Engineering Doctorate scheme, which include five project related submissions, the International Placement Report, the Personal Profile and the Innovation-Report.

1.4.5 Adhesion Effect (Submission five)

Submission five reports the investigation to simulate the soiling process under laboratory condition. As stated after the literature review, a correct replication of the process needs to encompass not only the sedimentation of particles, but also the condensation process and repeated individual soiling events needs to be incorporated into the experimental work. Finally, the necessary particle removal force has to be analysed.

1.4.6 Innovation–Report (Submission six)

see 1.5 Innovation–Report (structure)

1.4.7 International Placement (Submission seven)

Despite traveling restrictions during most of the project, due to COVID an international placement in Almeria, Spain was conducted. Both research organisations, CIEMAT, Spain and DLR, Germany provided a place for shared work, experiences and the interest for future cooperation. Submission seven is reports on the experience made during the international placement in PSA (Spain).

1.4.8 Personal Profile (Submission eight)

The author's personal development during the period of the Engineering Doctorate program, was highlighted in Submission eight. Events such as conference presentations, meetings with international soiling group and the international placement in PSA (Spain) provided external opportunities to improve the author's communication skills and other key competences.

1.5 Innovation–Report (Structure)

The Innovation–Report (Submission six) represents a summary of the whole project, it highlights the main outcome of the project, and it's significant in the broader sense of the maintenance of solar collectors and gives a suggestion of future work. The document is divided into seven chapters, which states the importance of CSP, and the importance of the maintenance the solar collectors and optimisation of the research technique. The individual chapters are described as follows:

1.5.1 Chapter 1: Introduction

This chapter provides an overview of this thesis, its structure and the outcomes of the overall project. It summarizes the innovative aspects of the work and finally the publications attributed to it.

1.5.2 Chapter 2: Project and Methodology

The project motivation in a broader view and the applied methodology of the entire work is highlighted in this chapter.

1.5.3 Chapter 3: Soiled Mirror Sample Preparation

This chapter is focused on the development of an artificial soiling test rig, which replicated the soiling process under laboratory conditions. It also highlights progress made on the development of such rig in the past.

1.5.4 Chapter 4: Basic Reflectance Model

The opportunity to exploit the capability of the artificial soiling test rig is reported in in this chapter. This part provided a new approach on the reflectance versus soiling load description.

1.5.5 Chapter 5: Adhesion Force Analysis

This chapter highlights trials to replicate the natural soiling process and assess the created adhesion forces of the soiling material as bulk material.

1.5.6 Chapter 6: Discussion

A discussion and interpretation of the experimental work regarding their influence in the soiling aspect of the CSP operation, is highlighted in this chapter.

1.5.7 Chapter 7: Conclusion

This chapter presents of all major results and findings.

1.6 Innovation

This project was carried out in the framework of the Engineering Doctorate scheme, which was dedicated to optimizing the experimental method of maintenance issues encountered in CSP solar mirror soiling of CSP. Experimental methods which provide reproducible and robust results and replicated the soiling process as accurately as possible were required. This project also took the opportunity to work with the developed tools and methods.

Therefore the following points, as results of the conducted research, highlight the contribution to knowledge and innovation in engineering:

- A novel concept of an artificial soiling test rig for the preparation of soiled mirror samples. The concept and design of the new capability to perform sequential soiling tests for a specific mass deposition density without interfering effects to the previously soiled substrate. The test rig has the potential to integrate further functions, if necessary. This test rig provides a better prepared soiled mirror sample for experimental work in research and engineering when optimizing soiling and cleaning process for future solar operations.

- New empirical model of the reflectance of a solar mirror, which uses an exponential model, rather than a linear one. Differences between both models can be observed at relevant reflectance level for CSP. Furthermore, the basic reflectance model was enhanced with soiling material (mineral particle) specific parameter (size), and therefore highlighted a way to simulate reflectance from constituent parameters. The theory of soiling was presented by a numerical simulation, which proved the fundamentals of the model. The empirical model has the potential to predict reflectance of solar mirrors much more accurately and thus allows the avoidance of several cleaning runs per year, which reduces water consumption and the maintenance cost of a CSP operation.

- The project also presents a practical approach to replicate the natural soiling process, by repeatable soiling and condensation of mirror samples. These sequences were finished by dry phases, which influences the adhesion effect significantly. From literature, similar experiments were carried out, however not in a natural manner over several soiling events. It is assumed that a practical test procedure close on the natural effect experienced in the field would provide better results.

1.7 Contacts to the Research Community

1.7.1 Conference

The artificial soiling test rig was presented by the doctoral candidate at the SolarPaces conference 2021. Travel restrictions at the time owing to COVID

made it necessary to hold a video conference. Several relevant fellow researchers from the area of interest, presented at the four day conference.

1.7.2 Papers

The candidate as author:

- “Artificial Soiling Method and Test Rig for Solar Power Related Research” (Conference paper, accepted 2021)
- “Basic Reflection Model” (Journal paper, in preparation)

The candidate as co-author:

- “Cleaning concentrating solar power mirrors without water”, doi.org/5.0028557, (conference paper, 2019 published)
- “Variability and associated uncertainty in image analysis of soiling in solar energy systems”, Leonardo Micheli, International soiling group, (Journal paper, 2022 published), corresponding author

1.7.3 Poster

“Cleaning mirrors with low water consumption for concentrated solar power” presented at the SMM-CDT conference London, 2022

1.7.4 International Soiling Group

The candidate is a member of an internationally organised group of fellow researchers, all involved in soiling research of solar power applications, (Submission eight).

2 Concentrated Solar Power Technology and Research

This section describes the motivation for this project, which has its origin based in energy from sustainable sources. It is focused on the basics to maintain this energy source, the techniques, methods and equipment to optimise maintenance processes for efficient use of the investment for concentrated solar power.

2.1 Energy Demand for the Future

The energy demand (thermal, electrical and for transport) has a direct connection to the development of humanity in particular the less developed countries. The original approach of economic growth is that it automatically leads to improved standards of living for all humans. However, it was highlighted back in the 1980s, that future improvement of lower developed economies in connection with the population increase has devastating results on the three key areas of sustainable development, Economic-, Environmental-and Social Sustainability.

This was highlighted in the UN published report “World Commission on Environment and Development” (1987) [1]. It highlights the danger of natural resources by extended air-pollution, deforestation and potable water. Land loss, used for fishery and farming is visible [2]. Furthermore, climate change, lack of free potable water, soil poisoning and resistance against infectious pathogens are associated aspects of sustainable development.

It becomes obvious that all those Sustainable Development issues requires additional energy, more than currently consumed. Reference [3, 4] highlights the expected increase of future energy demand by comparing energy per capita consumption of developing countries with those assumed developed, e.g. USA.

2.2 Sustainability in Energy Supply

The expected future increase of the energy demand becomes steadily an issue, as well as the environmental problems associated. Therefore, sustainable (endless and free supply) and environmental clean energy sources becoming important for global energy supply. Reference [5] pointed to the unique

opportunity for Nigeria, which has the ability to provide a sustainable energy source to improve the economy and standards of living for all.

Massive increase of global CO_2 emissions 40% compared to pre industrial level [6], and the associated climate change [1, 7], makes a change of primary energy sourcing necessary, they are carbon based [8, 9]. Furthermore, the expected increase of energy demand, due to the standard of living and population increase adds to the demand for sustainable and environmental friendly energy sources for the future [1]. Figure 2 shows he increase of global CO_2 emission and the forecasted energy demand.

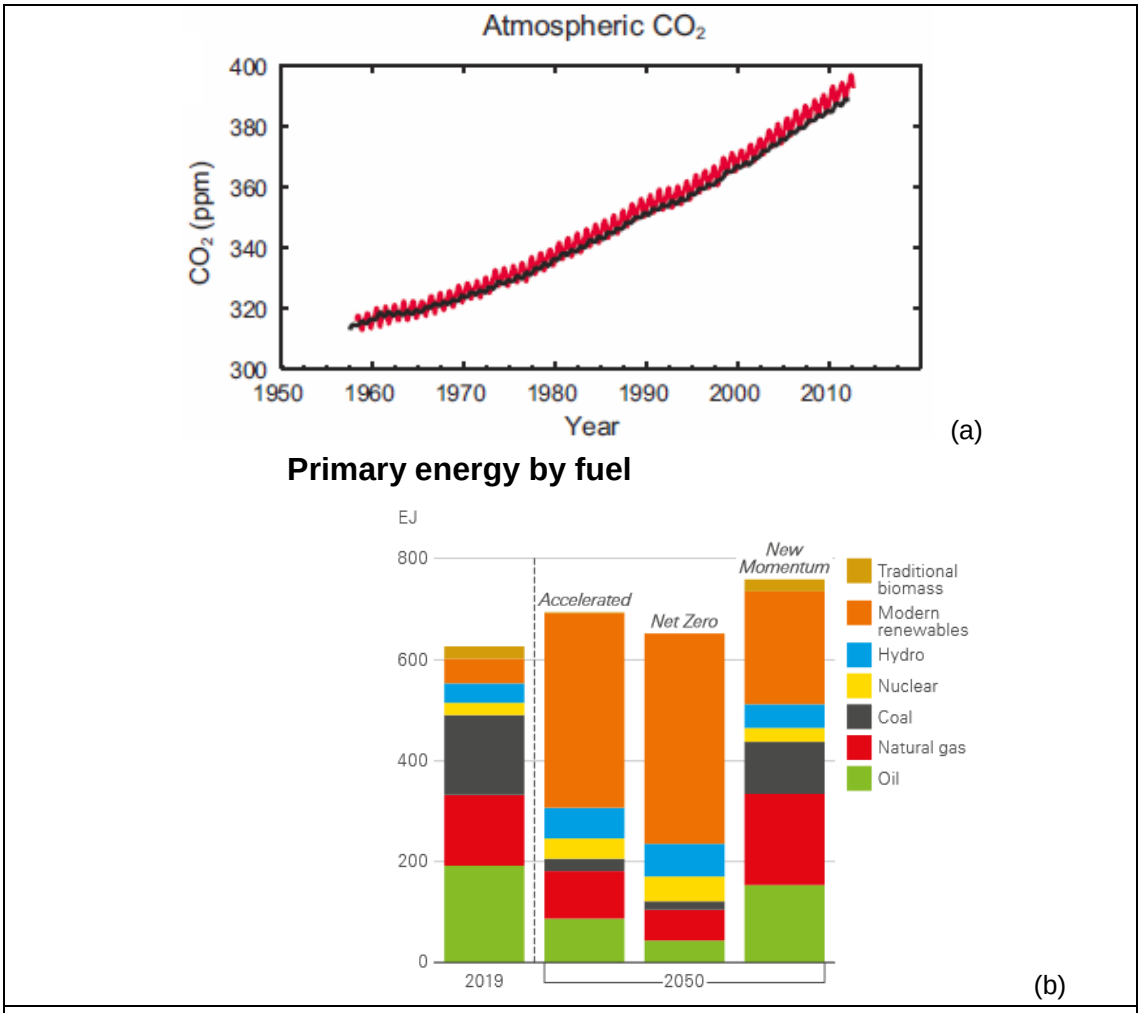

Fig. 2: Illustrations of total CO_2 emissions, a) from the period 1950 to 2010 and b) primary energy demand (fuel type) by 2050 (*). Source: [6, 10]

Note: (*) Two scenarios (Accelerated and Net Zero), which assume the implementation of tougher policies and sustainable energy on two different levels, and one scenario (New Momentum) which assume a closer development on the current situation.

A further aspect of CSP is the direct production of the most used and suitable energy form, thermal energy. Statistics from Europe and Germany [11] highlights that the biggest fraction of Total (global) Final Consumption (TFC) is thermal energy and it is assumed that the global distribution is not much different. Figure 3 shows diagrams for the TFC distribution in Germany and Europe [12]. This highlights the importance of thermal energy as a primary and secondary energy form, which can be serviced by solar energy (which is sustainable energy source).

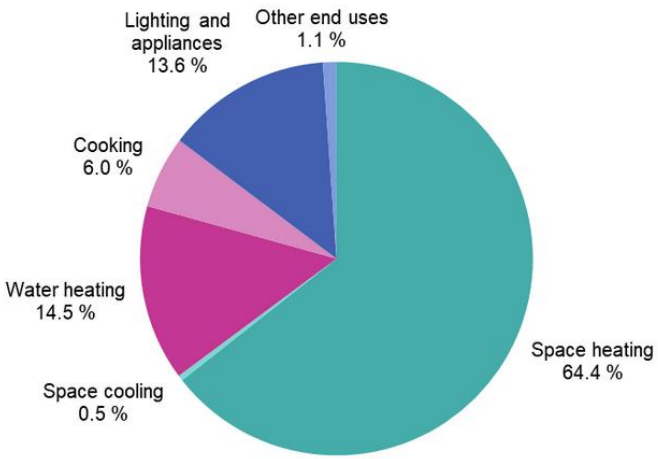

Fig. 3: Final energy consumption in the residential sector by use, EU, 2021. Source: [12]

The supply of thermal energy directly from relevant renewable energy sources, is a proven technology with further potential for optimisation [13, 14]. Solar thermal energy, and in particular CSP has exceptional large commercial potential, due to a wide variety of applications and low associated costs [2, 15, 16].

2.3 Concentrated Solar Power (CSP)

Renewable energy supplied from CSP, wind, biomass and photovoltaic panels is becoming an increasingly important sources of energy for the future with a commercially potential [16]. CSP “harvests” radiation from the sun to use it either directly (heat for industrial operations) or transforms it in electricity via

conventional steam turbine technology [17]. It is obvious that this technology offers endless available energy resources for mankind. In addition, CSP is suitable for sunlight rich regions, e.g. deserts and arid areas [18, 19]. Every square metre of the Sahara desert receives solar energy > 2,000kWh of every year or the equivalent to 1–2 barrels of oil in the same time [20, 21, 22].

These applications are working on the same principles, where direct solar radiation is collected over a larger area, reflected by a solar mirror to a focus point (or line), in which a medium (water, oil, gas or air) is being heated up; depending on the mirror area [23]. For the focusing solar radiation it is only direct irradiance suitable (not diffuse radiation as in photovoltaic) [19]. In addition, Thermal Storage technology provides the capability to operate the power plants during the night.

Parabolic trough collectors consist of parabolic shaped solar mirrors fitted around their centrally-mounted absorber tube. A one axis tracker system follows the sun direction for a better reception of the sun's radiation throughout the day [24]. An absorber tube is located at the focus point/length of the solar mirror, which covers the "energy transfer-medium" (water or oil, depending on the operational temperature [24] Table 1.

Fresnel collectors have a series of narrow "mirrors strips", which are rotatable along their length axis, which creates a Fresnel mirror (in this way, a degree of "curvature" can be achieved from essentially flat sheet mirrors). Due to rotation, the "mirror strips" are constantly aligned to the current sun position. This "mirror bench" reflects the sunlight to the absorber tube, which is assembled in the centre of each "mirror bench" to a height of around 7m. The Fresnel collector is easier to manufacture (being flat in profile) and more cost effective compared to the parabolic trough collector. For further details see Table 1.

The parabolic dish collector is a 2D, parabolic and concave shaped solar mirror (two axis system), which reflects the sun radiation to the central focal point. A two axis tracker system follows the sun position. This very high efficiency system [25] operates with a receiver device (helium gas, 650°C) or an integrated (Stirling engine) see Table 1.

The solar tower plant (Heliostat) design uses a central tower with the receiver device, which is located in the centre of the solar field. Multiple reflectors (heliostats) with flat solar mirrors, are arranged around the tower, with each having a two axis tracker system [8]. The total of all reflective solar mirrors collectively create a two dimensional Fresnel mirror see Table 1.

Figure 4 shows four representative CSP collectors, (a) parabolic trough collector, (b) Fresnel collector, (c) Heliostats and (d) parabolic dish collector**.**

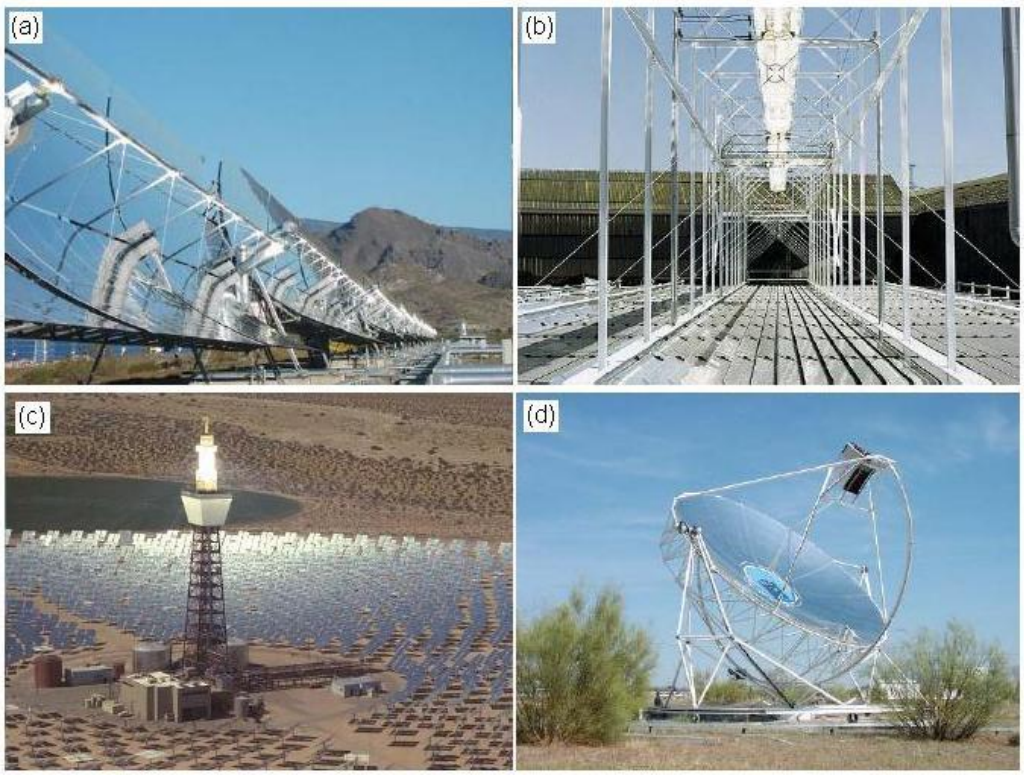

Fig. 4: Different CSP collector types, (a) parabolic trough collector, (b) Fresnel collector, (c) heliostats and (d) parabolic dish collector (with Stirling engine).
Source: public domain

Solar collectors are sorted according to their temperature output. CSP operations using medium and high temperature collectors, where medium temperature collectors are dedicated to process heat operations. Low temperature applications are commonly used for domestic and small business applications due to cost and safety [26]. Higher temperatures can be achieved by a higher

concentration (Concentration factor, C_r), of the sun radiation. Concentration factor (C_r) expresses the ratio of the aperture area (receiving mirror surface area) to the absorption area on the receiver device [17, 19, 27]. Figure 5 highlights the influence of C_r on the achievable temperature output.

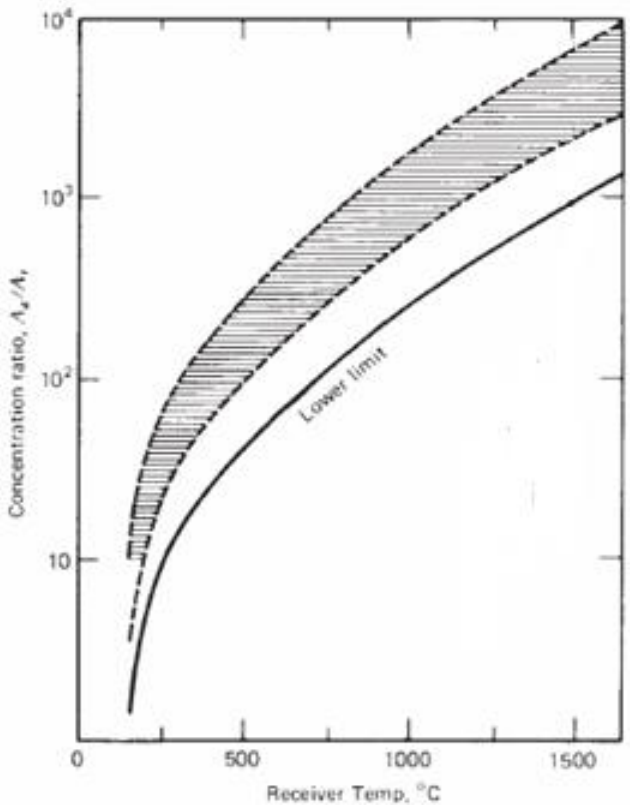

Fig. 5: Dependency between concentration factor and output temperature.
Source: [26]

Table 1 highlights the major solar collector types (low, medium and high temperature), with their main parameter (e.g. temperature classes).

Table 1: Solar collector type, and their temperature range and Receiver device [19, 24, 26, 27, 28].

Temperature Class:	**thermal Solar Collector Type:**	**Concentration–Ratio (Cr) and (op. Temp)**	**Receiver Device:**
(1)	(2)	(3)	(4)
low Temperature (< 190°C)	flat plat collector	< 1 (27-77°C)	simple tube receiver or
	evacuated tube collector	< 1 (47-187°C)	evacuated tube (linear receiver)
medium Temperature (240-510°C)	Fresnel collector	10–40 (67-270°C)	receiver tube (linear receiver)
	parabolic trough collector	15–40 (47-400°C)	
high Temperature (> 550°C)	parabolic dish collector	100–1,000 (47-950°C)	central receiver unit (point receiver)
	Heliostats	100–1,500 (130-2,727°C)	

2.4 Maintenance aspect of Solar Collectors

CSP technology requires an efficient magnitude of Direct Normal Irradiance (DNI) in order to work economically. By experience, a DNI of up to > 2,000kWh/(a x m^2) is required for a CSP operation [22, 27, 29]. The majority of the solar radiation reaching the atmosphere, will get lost, because of aerosols (air pollution, moisture and atmospheric content) [19, 27]. The path length of the solar rays through the earth's atmosphere (expressed as air mass) also influences the final DNI, which reaches the solar collector [19, 27]. Globally, desert, arid and semi-arid regions provide constantly high DNI. Figure 6 shows preferred regions for solar collectors globally.

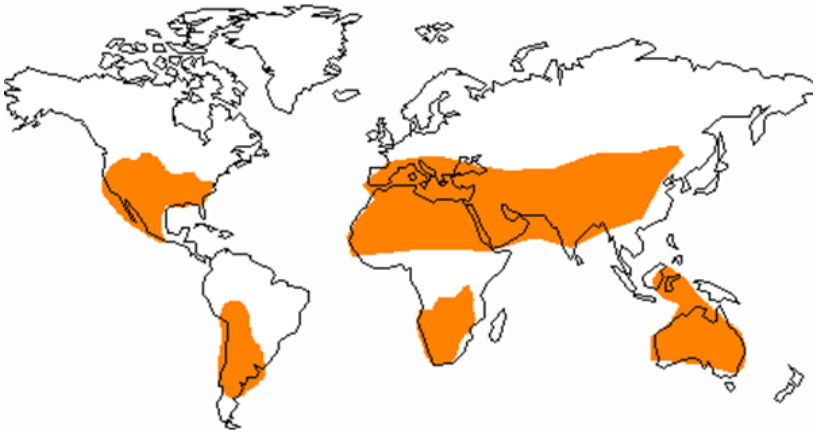

DNI > > 2,000kWh/(a x m^2)

Fig. 6: World map of high Direct Normal Irradiance, [kWh/(m^2 x a].
Source: [29]

The preferred areas for CSP also provide a high soiling effect from mineral particles and other aerosol sedimentation which collect on the collector component's surfaces, including the solar mirror, solar lenses, transparent covers and receiver devices. The soiling effect causes performance losses and reduces the reliability of operation [30, 31, 32]. The visible effect of different soiling materials, can be seen in Fig. 7. Be aware, that most of the sources referenced, report on PV-cell soiling, however the basics issue is the same for CSP soiling.

Fig. 7: Examples of intense soiling material of different types, (A) mineral deposit, (B) bird droppings, (C) biofilm of bacteria, algae, lichen, mosses, or fungi, (D) plant debris or pollen, (E) engine exhausts or industry emissions, and (F) agricultural emission e.g. feed dust. Source: [33]

Note: Transmittance will be not mentioned, however soiling as described has the same negative effects on the transmittance characteristics.

The extension of the expected power losses, can be more than 1% reflectance per day, which leads to a performance loss of up to 10% in a period of two weeks [34] Fig. 8.

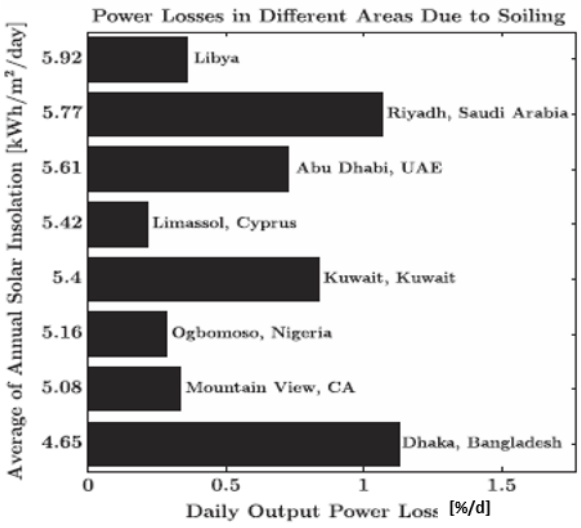

(a)

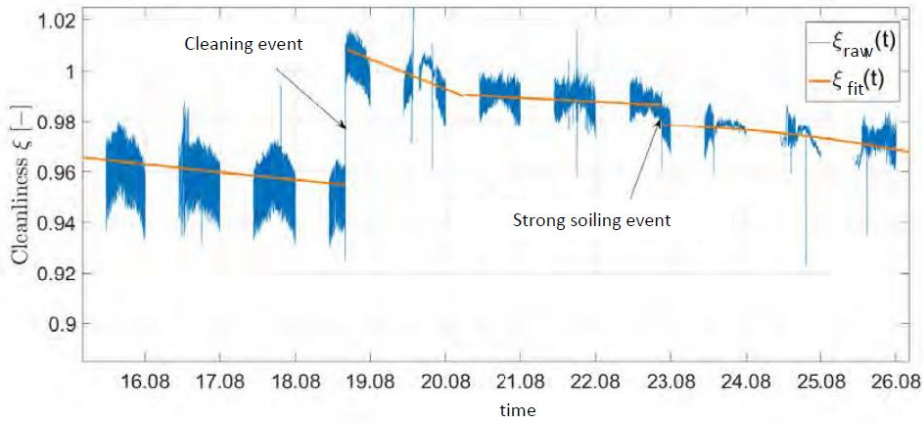

(b)

Note: No statement of solar collector type.

Fig. 8: Diagrams of (a) power losses [%/d] due to soiling from eight representative locations and (b) normalized reflectance (Cleanliness) data over a period 11days. Source: [30, 35]

Note: Soiling rate is often defined as power-loss, (or efficiency loss) over time [%/d or 1/d].

The total solar collector efficiency is also dependent by its optical efficiency (η_{opt}), which is in relation to its specular reflectance (ρ) besides other parameter such as transmittance (τ) and absorbance (α), see Eqn 2-1 [19, 27]. The total collector efficiency (thermal energy output) is directly dependent from the mirror reflectance capability. Furthermore, the direct economic influence (maintenance cost, L_{tot}) of the mirror reflectance is highlighted in Eqn 2-2, [36].

Optical Efficiency:

$$\eta_{opt} = \Gamma \cdot \rho \cdot \tau \cdot \alpha \qquad \text{Eqn. 2-1}$$

and Maintenance Cost:

$$L_{tot(t)} = (\rho_0 - \rho_t) \cdot \int_t^{t+1} p_{(t)} \cdot DNI_{(t)} \cdot \eta_{(t)} \cdot dt + C_{cl} \cdot A_k \qquad \text{Eqn. 2-2}$$

Note: The capture fraction (Γ) is a number, which descripts the mirror shape quality and the relevant receiver size. The capture fraction is also used to highlight the reflected energy which does not reach the absorber surface.

2.5 Solar Mirror Cleaning Methods

Commonly, cleaning methods for solar mirrors are demineralized water (water of hardness < 12ppm and with an agent) based methods, which only work with water spraying (non-contact types) and methods which uses water in connection with mechanical devices (contact types) [37].

Non-contact methods spray high pressure water (> 200bar) onto the soiled mirror surface with high effectiveness, it recovers up to 98% of the original reflectance [31, 38, 39]. Another method is Deluge Spraying, which has a higher water consumption however, this provides better results (up to 99% of the original reflectance) [37, 39].

Contact Cleaning utilises high pressurized water as well, however, this method includes additional tools such as brushes, to wipe or scrub [37, 39]. These methods have the advantage of up to 100% achieved reflectance compared to the previous “clean reflectance” value. Furthermore, these methods can damage the mirror surface (by scratches or delamination) [37].

Figure 9 shows example of contact cleaning and non-contact cleaning methods.

(a) (b)

Fig 9: Semi-automatic cleaning in CSP plants, (a) semi-automatic cleaning of parabolic trough collectors and (b) semi-automatic cleaning of heliostats. Source: [37]

Water Consumption of a CSP Operation for Solar Mirror Cleaning

The main fraction of the demineralized water (> 90%) on a CSP operation has traditionally been required for the cooling process [24, 39], but new development in cooling technology (air cooling) shifts the main fraction of water consumption towards the cleaning operation, which is assumed to become more dominant in the future [24, 39].

The actual water consumption and therefore production costs are mainly dependent on the collector's aperture area, which governs the solar mirror area. The receiver tube cleaning is not taken into consideration. The total solar mirror area is dependent on the maximum energy output (capacity) of a specific CSP operation and whether heat storage (HS) is in operation, these operations need additional aperture mirror area.

Specific Water Consumption

From literature [24, 35], on average, a $1m^2$ solar mirror area needs between 0.7–$1L/m^2$ (0.001–$0.00007m^3/m^2$) of demineralized water. This specific water consumption value is heat storage (*) independent. For the example of ANDASOL I plant, with a nominal capacity of 50MWe heat storage (HS) and $510{,}000m^2$ aperture area, an assumed $1L/m^2$ spec water consumption is made

[38]. Reference [35] is more specific and divided specific water consumption between technology and collector type, however the results are quite close to the mentioned figures described in [24, 35] in Table 2.

Table 2: Average demineralized water consumption for maintenance (cleaning) work on CSP operation.

Cleaning Method:	**Tower Plant** Heliostat [L/m$^{2]}$]	**Parabolic Trough Collector:** [L/m$^{2]}$]	**Ref.:**
Contactless Cleaning	0.85	0.75	[35]
Contact Cleaning	0.8	0.7	[35]
General	1.0		[24]

Note: (*) HS on a CSP operations are commonly molten salt storage tanks, which have the capacity to store additional thermal energy during daytime operation in order to provide energy in night hours for longer operation periods.

Water Costs

The demand for demineralized water and the associated costs and overall cleaning costs for solar mirror maintenance are highly location and plant-size dependent. Water costs vary according to the availability of the commodity. Reference [24] highlights between 4.0–0.03 EURO/m^3, depending on location. While the solar field La Africana (49.9MW) South Spain sources their water for 0.03EURO/m^3, Shagaya CSP plant (50MW. Kuwait) has a water cost of 4.0EURO/m^3 due to transport issues [24]. Total water consumption is dependent on CSP capacity (size) and cleaning period.

Total average cleaning costs for CSP are reported in [33], which include processing costs, labour and overheads. Figure 10 highlights the yearly total water consumption for common CSP field capacities and two cleaning periods (7days and 10days), Submission one. It also highlights the associated demineralized water costs based on the example of three different specific water prices, where the highest represents a very high price and the total cleaning costs.

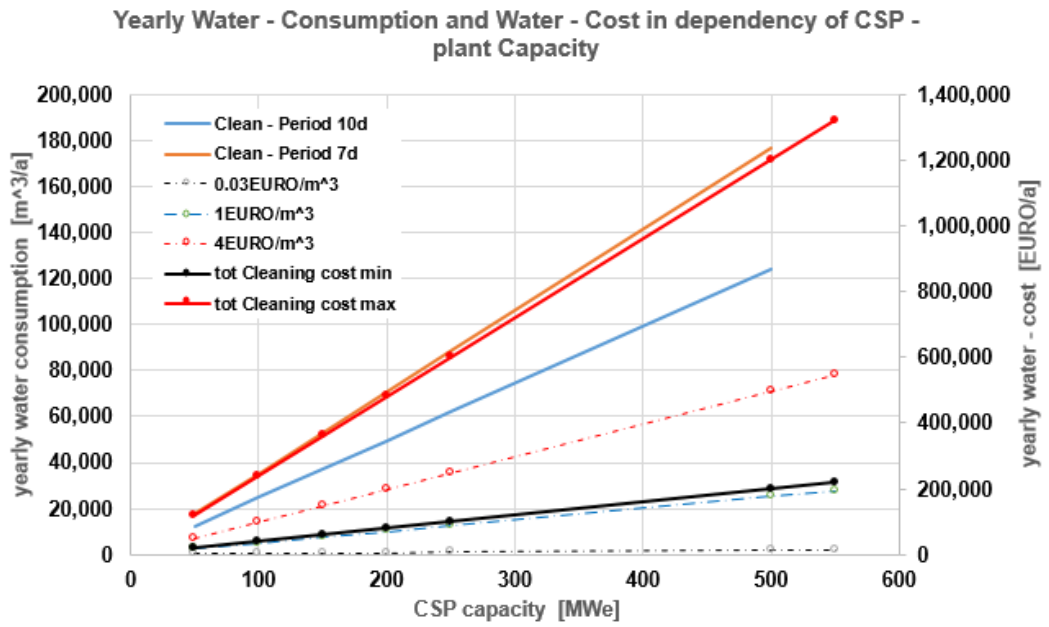

Fig. 10: Diagram of CSP capacity dependent water consumption and associated water cost in dependency of different water tariffs. Source: [33]

It can be clearly seen how the annual cost is rising with increasing capacity sizes of the CSP operation. In the year 2021, all globally operational, under construction and planned CSP capacity has volume of 9,500MW_e, which represents an aperture area of >76x10^6m^2 (Power Density 8,000m^2/MW_e). This highlights a global cleaning cost between 3.8–22.8 x 10^6EURO/a. Furthermore, when taking technologies such photovoltaic and evacuated tube collectors into consideration than it becomes clear that the collector maintenance and in particular cleaning is a business with potentially high growths, Appendix B.1 shows growth figures of CSP capacity and aperture area [39].

2.6 The need of constant Optimisation of Maintenance

It is obvious that constant optimisation of solar technology, in particular maintenance effort is necessary. This optimisation also includes research methods, which constantly have to adapt fundamental understanding, in this case soiling.

In the CSP case, cleaning costs is a global issue with large potential, which highlights the need of constant optimisation of the cleaning process. [24, 33]. This includes improved cleaning techniques, such as tooling and mirror surface manipulation which are constantly in the focus of research. Surface energy

adaption (hydrophilic and hydrophobic) has self-cleaning effects, which is under current investigation, [40, 41, 42].

In addition, field validation of future solar operations, highlights the issues of maintenance and soiling mitigation. Such an analysis includes effort and cost analysis, [43, 44]. Furthermore, soiling research projects extends to PV technology [45, 46, 47], even though there transmittance is the main parameter rather than reflectance. However it shows that the research community is also active in further development of the soiling process and constantly improving artificially replicating soiling effects under controlled laboratory conditions, which makes this research of importance [48].

2.7 The Project

The use of an atmospheric pressure plasma system in order to manipulate the surface energy of solar mirror surface to improve condensation collection on the mirror surface is currently a development of the sponsoring company ADTEC Ltd. This has the potential of improved self–cleaning characteristics, which could reduce cleaning effort [42].

This project, aims to improve and develop laboratory methods to simulate soiling natural situations, including condensation. Laboratory experiments have the advantage of controlled conditions, allowing repeatable tests and the option of isolating specific influences. These methods and equipment, will provide a tool to improved cleaning process experiments, e.g. evaluation process of equipment or CSP fields. However, exploiting and investigating the developed methods and the artificial soiling test rig when appropriate is also part of the project.

1. **Work Package 1 (WP 1)**
The artificial preparation of soiled mirror samples, repeatability to a required soiling load is an issue which is not satisfactorily solved, Submission three. Such an artificial soiling test rig is required for further soiling analysis.

2. **Work Package 2 (WP 2)**
Working and exploiting the artificial soiling test rig's potential, gaining experiences and working on the expansion of the basic reflectance model.

3. **Work Package 3 (WP 3)**
Developing method and execution of the replication of the natural soiling process, which includes sequential soiling and condensation. Validating the results and compare them with traditional methods.

3 Soiled Mirror Sample Preparation

To prepare soiled mirror samples (or glass samples) a soiling rig, which replicates the natural soiling process under lab conditions must be used (and firstly designed). The soiling process must be carried out holistically and repeatable and in addition, constant experimental conditions and parameters needs to be ensured.

An artificial soiling test rig is the tool, which has this capability. However, a test rig for repeatable soiling and soiling to a set target (which means to a pre-established and realistic soiling load over a given area) was not available from the literature. Therefore, an artificial soiling test rig with extended features (e.g. sequential soiling) was designed, developed and used in this research. A literature review (Submission three) highlights design concepts used in soiling research in the past. Repeatable soiling was not studied prior to the work detailed in this report, only “one off” soiling process test rigs were manufactured.

The international placement provided the opportunity to work on and analyse an unpublished artificial soiling test rig. The outcome will be highlighted together with an improved test rig concept, below in the chapter Discussion and further work.

In addition to the experimental work health and safety measurements are also of importance. The relevant legislation was used in order to investigate the load of mineral exposure during laboratory work.

3.1 Methodology

The literature review highlights three major groups of concepts of artificial soiling methods suitable for the deposition of silt material onto a flat surface. A common approach was to use a liquid solution (water or acetone) mixed with silt material to form a suspension [49, 50, 51, 52]. Another group of methods suspended the mineral particles with pressurised air [53] and lastly, the use of gravitational force was also common. The soiling material was released at a certain height [54, 55, 56], down on to mirror sample’s surfaces. One design used a fine sieve to supply the soiling material, apparently achieving a better material distribution

[54]. One reference mentioned that the first group provides better soiling distribution while the gravity driven methods have a better soiling characteristic towards target soiling [54].

The artificial soiling test rig designed for the work detailed in this report is shown in Fig. 11a. This used the principle of gravitational force to feed a pack of soiling material into the upper opening of a glass drop pipe with an even distribution. The most important design feature, which is the capability of being able to repeat soiling sequences (as would happen in the natural environment), was guaranteed. This is because no feature of the release method (a “dry” method in connection with gravitation) interferes with the previously applied soiling material on the sample. The option of an individual soiling event as well as multiple soiling sequences were provided.

The mass of soiling material was precisely prepared in order to achieve the target mass deposition density (MDD, g/m^2), which represents the soiling load. The released mineral particles (silt) were distributed through a sieve with a fine mesh size (~ 63µm) and the help of a slowly exciting oscillating device. To improve the particle distribution, a relatively small sieve size (diameter: 20mm), compared to the soiling area (diameter: 70mm) was used. During the release process the sieve was above the upper drop pipe opening. This method allowed a longer release process, Fig. 11b. The particle dropped through the pipe (500mm long) on to the soiling area (circular area, diameter 70mm) in the centre of a 100 x 100mm, 1mm thickness mirror sample. The mirror sample were located on the lower opening of the drop pipe. The particles needed an extended time period to settle. According to the Stoke equation, a period of ~ 60min would be required, however authors [57] revealed that 30min would be sufficient. Therefore, the total mass of the mirror samples was measured after > 30min settling time, and compared with the mirror sample mass (clean). Mass deposition density (MDD) was then calculated by dividing the soiling material mass by the soiling area.

Mass Deposition Density (MDD) represents the particle mass per mirror area in [g/m^2] [50]. Commonly MDD is stated to one digit after the decimal point. This mass related parameter does not directly correlate with reflectance as it is dependent on overlapping and optical properties of the deposited material itself.

Figure 11a, b shows the artificial soiling test rig and the release device on the upper drop pipe opening. Figure 11c, d, highlights two soiled mirror samples

(MDDs of 1 and 2.8g/m^2 respectively). Note that Fig. 11d presents a soiling example of a smaller soiling area (32mm), this feature became necessary to improve particle distribution at high soiling load (MDD > 1g/m^2). Further images of the artificial soiling test rig are given in Appendix B.2.

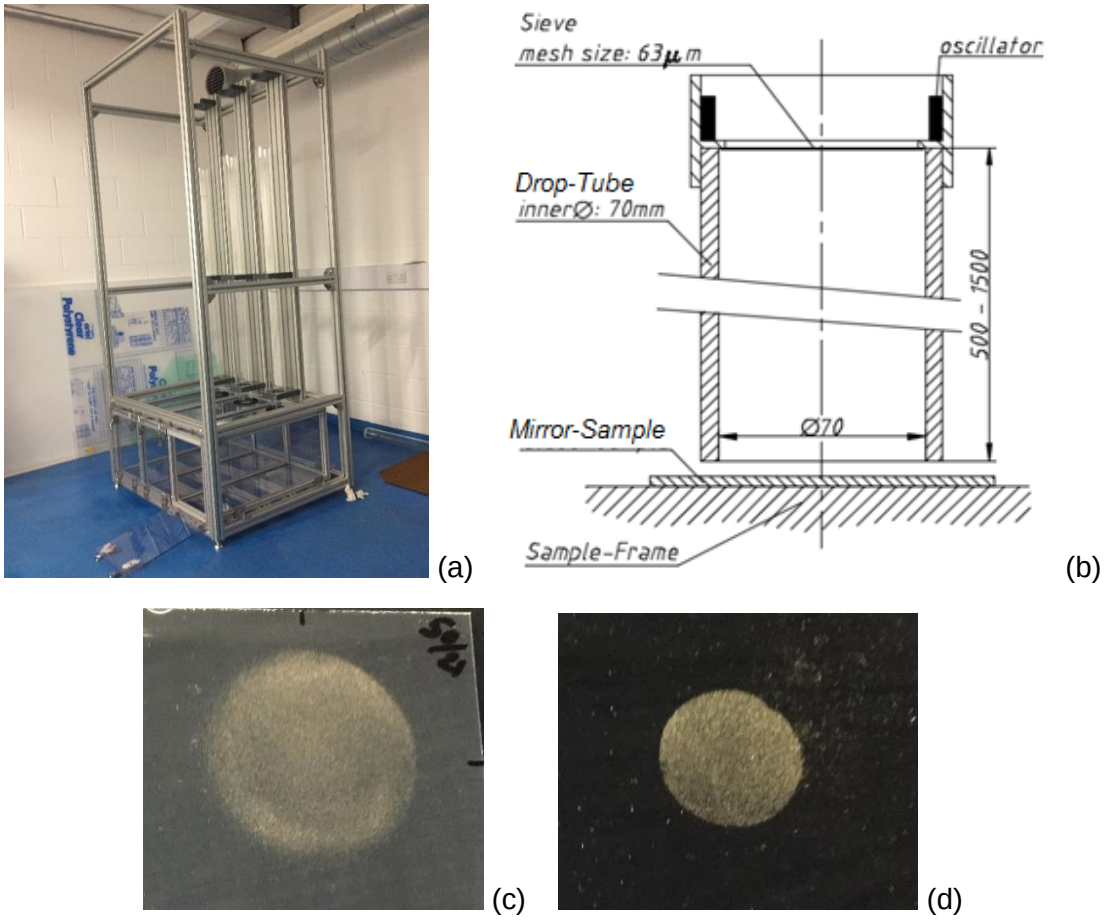

Fig. 11: Photos of the a) artificial soiling test rig. b) drawing of the main components and soiled mirror samples with c) MDD: 1.0g/m^2 (70mm), d) MDD: 2.8g/m^2 (32mm).

Finally, the average specular solar weighted reflectance (RSe) was measured on five locations of the mirror sample. A measurement jig was manufactured specifically to provide an efficient and precise measurement process, which yielded a repeatable of a measurement location with a tolerance of +/- 0.5mm (by observation).

All experimental soiling work used mirror samples supplied by AGC-Glass Europe, High clarity low iron float glass (DIN EN 572-1, DIN EN 572-2), 100 x 100mm, thickness: 1mm, uncoated, and soiling material (silt material, comparable with ASTM-C33-99a, dry) and a particle size < 63μm (sieved, mesh size). The investigation process analyzed the mirror samples soiling repeatable (MDD) and with uniform soiling material distribution (average specular solar weighted reflectance, RSe). These quality features are necessary as:

- Repeatability is important for sequential soiling and
- Precise uniform particle distribution for additional characterisation

The following lab equipment was used during the project used:

Soiling material mass measurements: laboratory balance (Sartorius CF 225D), which measured the particle mass to an accuracy of +/- 0.04mg.

Specular reflectance measurement: Reflectometer (ABENGOA, Condor 6LED, accuracy +/- 0.2%), [58]. Specular reflectance is dependent on wavelength, incidence angle and acceptance angle and is determined on the basis of six wavelengths (435nm–1,050nm). The final value of average specular solar weighted reflectance (RSe) was determined according to ISO 9845, [59]. Specular reflectance (RSe) is a ratio and therefore without a unit, throughout this report the symbol “[1]” is used for RSe.

A soiling load in the range of MDD between 0–2.5g/m^2, was used for the initial tests. According to [35] most CSP operations are accepting a RSe of > 0.9[1] reflectance, however some operations reported ~ 0.85[1] [60]. Therefore, this project choose a specular reflectance range from (clean) 0.964[1] to 0.75[1], which is the equivalent to MDD 2.5g/m^2. Also, this project used absolute reflectance value and not normalized (cleanliness) values. Only one batch mirror samples was used and therefore comparisons between different solar mirrors were not carried out.

3.1.1 Operational Procedure

The provided Standard Operational Procedure (SOP) can be seen in Submission three and will be not explained here in detail. However, the biggest hazard for the soiling experiments was the exposure to fine dusts, which the operator will inhale automatically unless protected. The situation becomes dangerous due the fact that partly used silica minerals (crystalline) were being used, which is to some extent in all mineral samples included, which could have toxic and lung tissue damaging consequences.

Therefore the process had to be analysed according to the Workplace Exposure Limits (Health and Safety Executive, HSE) [61], which are relevant for UK operations and deals with the exposure limits.

The executed analysis assumed the worst case scenario, which means 100% (realistic 95%) silica (quartz, crystalline), and therefore being respirable [62]. Twelve samples were soiled in a period of 8hours. The lab has a volume of > $50m^3$ (realistic > $100m^3$) and one sample has a time process period of 15min [50]. Furthermore, the maximum MDD is soiled (MDD: $3.0g/m^2$), which requires 11.2mg soiling material and additionally ~ 6mg dust (50%) is lost during the process.

This will not exceed short term ($0.24mg/m^3$) and long term ($0.08mg/m^3$) dust concentration limits [61]. This would be the equivalent of more than 20 samples/8h and realistically 12–15 samples could be processed during an 8h period, Submission three. Therefore, the use of a class 3 fitted Face Fitted device was not required. It was assumed that keeping the lab safe from mineral exposure, regular wet cleaning would be required.

3.2 Experimental Results

An extended test series analysed the repeatability of the soiling process, when soiling each mirror sample to a specific target MDD. The difference between the real soiling load or experimental MDD and required MDD or target soiling load will be analysed. It was not expected that the test method used produced the exact target soiling load. The discrepancy is related to the preparation process of the soiling material pack. In order to compensate the difference partly, the soiling material pack was always “over soiled” rather than “under soiled”. More soiling material was prepared than required, which is called “theoretical” MDD.

Figure 12 presents the results of the repeatability test - series, which includes five groups of one target MDD value each. Theoretical MDD values are highlighted against their experimentally achieved MDD value. The red line represents the equal results level, meaning that theoretically achievable results were measured. The mentioned effect of “over soiling” can be seen as a horizontal off-set from the nominal target MDD value.

The discrepancy between the theoretical and measured value is the vertical distance between the data point and the red line. The linear correlation of the

measured MDD data is highlighted in Fig. 12 as black (MDD <4g/m^2) and blue (MDD <2.5g/m^2) on lines.

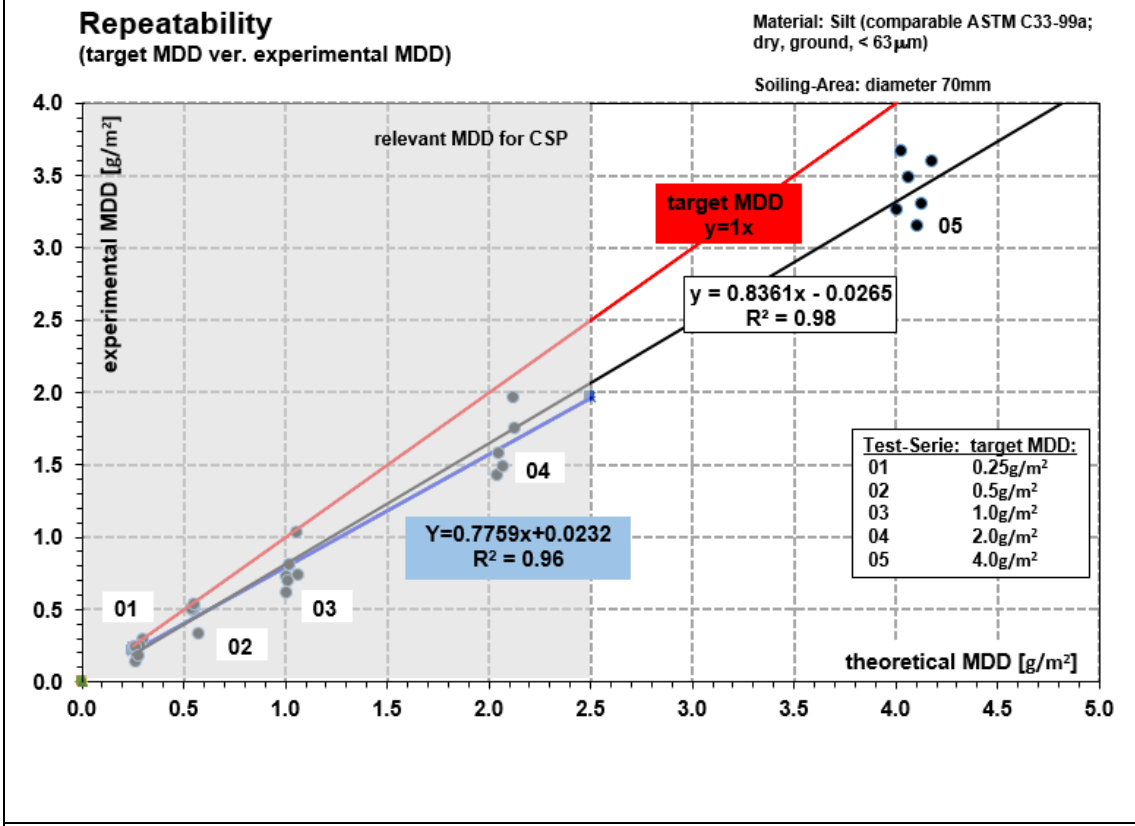

Fig 12: The correlation between the theoretical MDD and experimental MDD, including the target MDD.

The artificial soiling test rig can be seen to provide consistence results, which are not identical to the target MDD value, however the error is predictable. The linear correlation has a R^2 coefficient between 0.98 and 0.96[1] defined as a total MDD range and 2.5g/m^2 range respectively. The linearity highlights that an equal proportion of the prepared soiling material gets lost during the soiling experiment, which is in the range of 16.3% to 22.6% (total MDD range and 2.5g/m^2 range respectively). Most of the losses of soiling material, during the soiling experiment are related to electrostatic charges of the inner surface of the drop pipe, which become visible after several soiling tests. Washing with deionized water within every 2h reduced this effect to an acceptable effect.

Further test series highlighted the correlation between the soiling load parameter MDD and average solar weighted specular reflectance (RSe). The RSe values

of target soiled mirror samples were measured and plotted against their MDD value.

Figure 13 presents the relationship of the soiling load (MDD) and the specular reflectance.

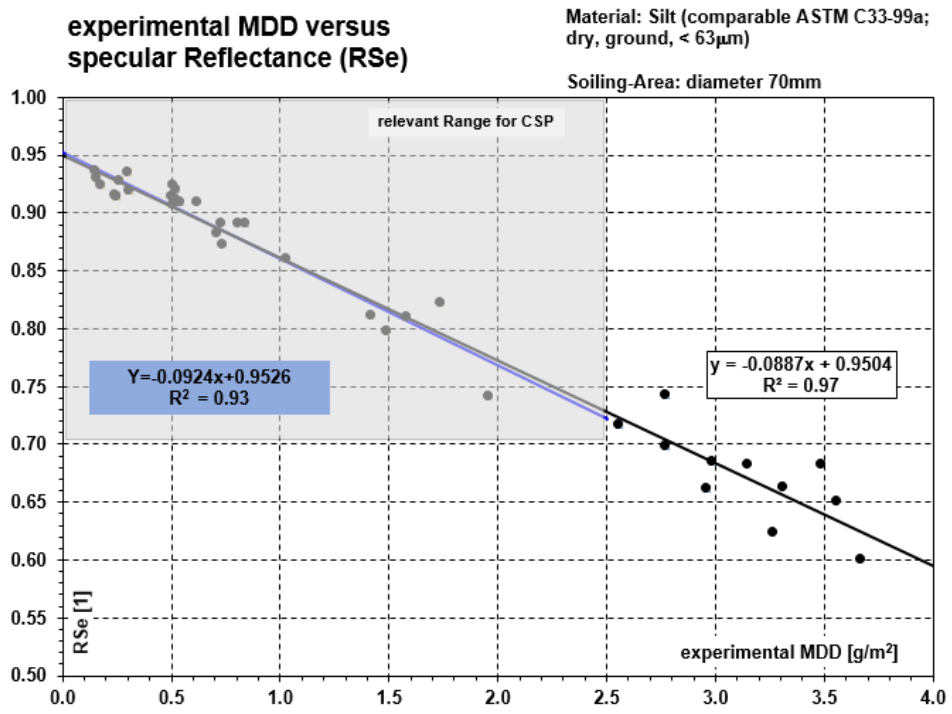

Fig 13: Correlation between experimental MDD and specular reflectance.

A high consistency of the values and correlation coefficient (0.97[1] and 0.93[1], total range (< 4.0g/m^2) and CSP range (< 2.5g/m^2) respectively) highlights a good and consistent soiling process provided by the test rig.

The equal deposition of soiling material was tested by analysing the specula reflectance distribution on five locations (one in centre and four equally distant to centre) of the mirror sample surface.

Several groups of mirror samples with one target MDD, had up to six individual sample repetitions carried out. Average reflectance and the standard deviation represent the discrepancies to an equal particle distribution. The std. deviation value of RSe represents a value range (+/- one standard deviation), which

includes 66% of all measurements. Figure 14 highlights the std. deviation, average value, maximum and minimum values versus MDD of each target soiling load group.

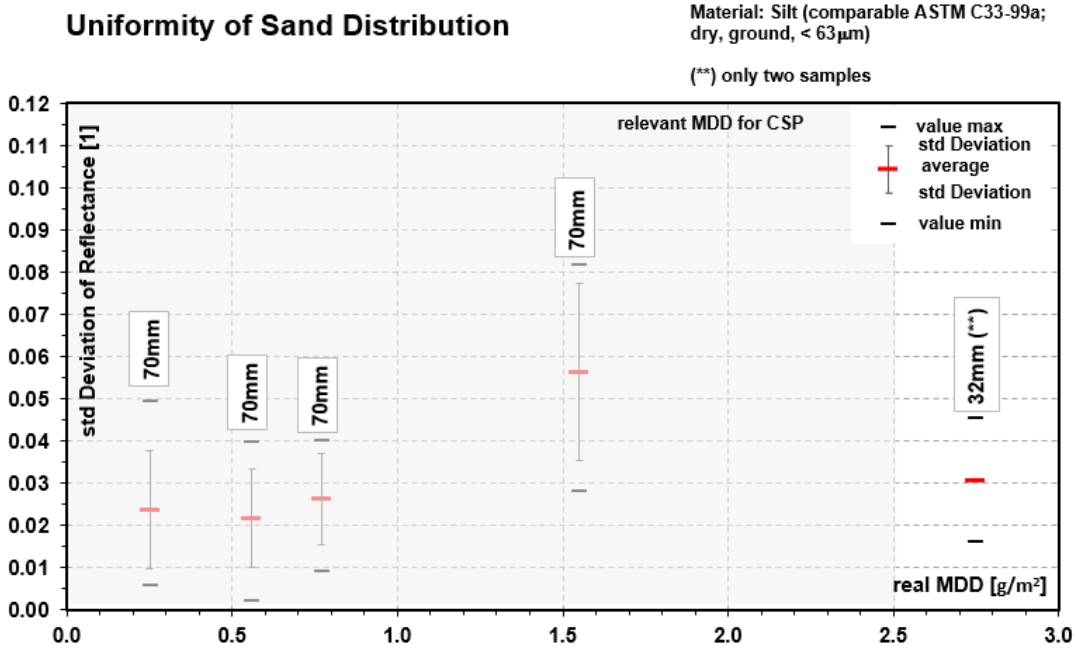

Fig. 14: Silt material distribution on soiling area of 70mm and 32mm diameter.

In total, mirror samples with a low soiling load (~< 1.0g/m^2) experience a better distribution of the sediment particles having an average span of 0.024[1], when beyond this threshold the RSe difference has a span of 0.05[1] Fig. 14. The analysis of the std. deviation shows a similar picture. From less than 0.015 to greater than 0.02[1] at the same MDD range (below and above 1g/m^2). However, a decrease of the soiling area from 70mm to 32mm has an improving effect, which compensates for the loss in accuracy, as can be seen in Fig. 14 right end. It is assumed that the centre of the soiling area is easier and more consistent to soil rather than areas towards the edge. Reducing the edge area (by masking) results in a more equally distributed soiling zone. At lower MDD values, the difference between the centre and edge is not as visible as at higher MDD values.

The capability to soil a mirror sample repeat ably was tested further. Three test series were conducted, each with a target MDD of 0.25g/m^2 soiling run, where a total of 10cycles was carried out. This procedure represented a cleaning period of 10days (average soiling rate -0.1[1]/d [30, 35], with a soiling load of 2.5g/m^2 (0.75[1]). The soiling load applied was relatively high, however the test rig provided a robust soiling results at this MDD level.

Figure 15 shows all three test series (blue, red and black data plots), which are relatively consistent.

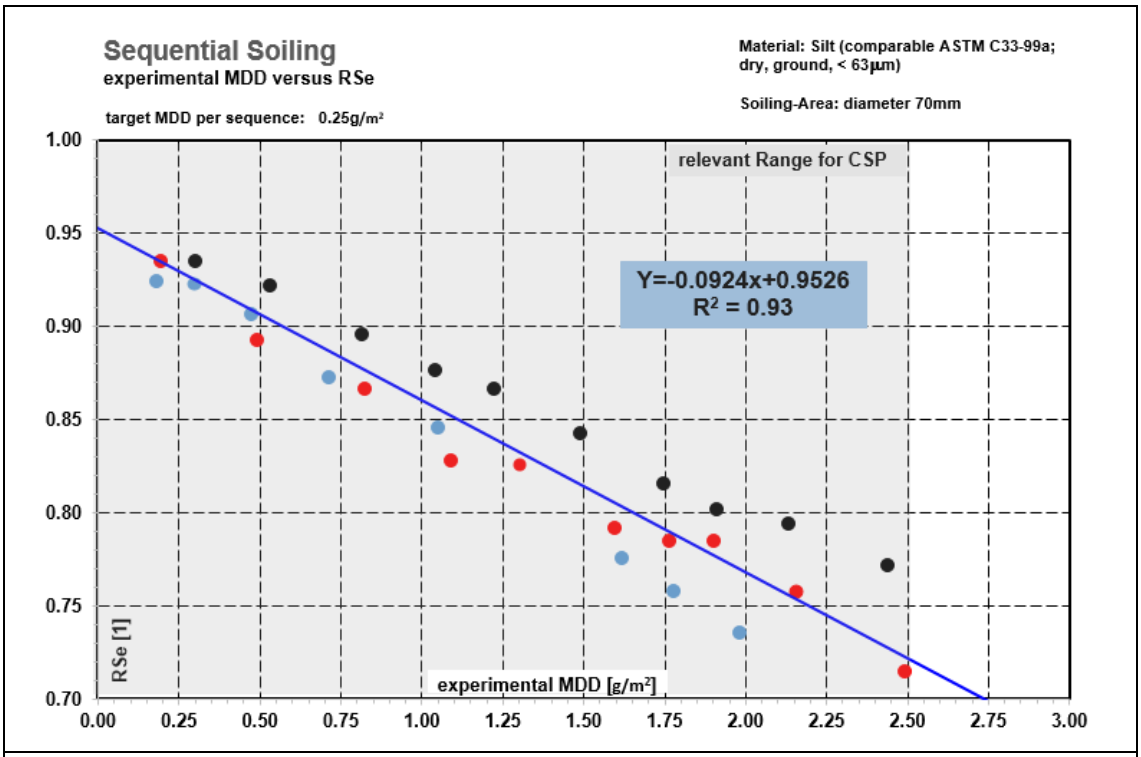

Fig. 15: Reflectance data of three sequential (MDD; 0.25g/m^2) soiling test series, with a final soiling load of MDD: 2.5g/m^2.

The three RSe values at the end of the test series have a difference of up to 5.7 (or absolute 0.04[1]) (blue line, Fig. 15). Future work include further improvements of the robustness of the soiling process and have the potential to improve the repeatability of sequential soiling.

4 Basic Specular Reflectance Model

The artificial soiling test rig (Submission three) was extensively used for soiling experiments, which ware targeted to explore the basic reflectance of solar mirrors in relationship to soiling load. Numerical simulation was used to provide extra proof of the soiling processing theory. Also the parameter “soiling load” was extended in order to express the “soiling intensity” according to reflectance influence (coverage ratio).

4.1 Soiling Theory

The project assumes the process of natural soiling as evenly randomly distributed spherical particles on a flat horizontal surface. The solar radiation, which is not reaching its required place (receiver device) is regarded as lost and therefore not a desirable occurrence. The performance of the solar mirrors is expressed in specular reflectance (RSe), which gradually decrease with soiling load (mass deposition density, 3.1 Methodology) and coverage ratio. Coverage ratio (q) describes the relationship of the particles covered surface area to the total surface area and measures the primary blocking of solar radiation.

Two parameter are used to express the intensity of soiling load (a) mass deposition density (MDD, g/m^2) and (b) coverage ratio (q, [1]), the mathematical description can be seen as follows:

$$MDD = \frac{m_{soil}}{a_{soil}} \quad \text{Eqn. 4-1a} \qquad \text{and} \qquad q = \frac{a_{cover}}{a_{soil}} \quad \text{Eqn. 4-1b}$$

when (m_{soil}) is deposited mass and (a_{soil}) the total soiled area (usual 1m^2) and (a_{cover}) is the area covered by particles.

Mass deposition density is the ratio between particle mass and surface area and coverage ratio is the ratio between area covered by particles and surface area.

Solar radiation is blocked in two ways by particles, [63, 64], primary blocking (before entering the mirror) and secondary blocking (when leaving the mirror). Only one surface area unit is involved in primary blocking in the case of secondary blocking, two area elements are involved one where the beam enters the mirror and one which is blocked by a particle. Figure 16 shows the principle

of primary blocking (Fig. 16b) and secondary blocking (Fig. 16c) and normal reflected solar ray (Fig. 16a).

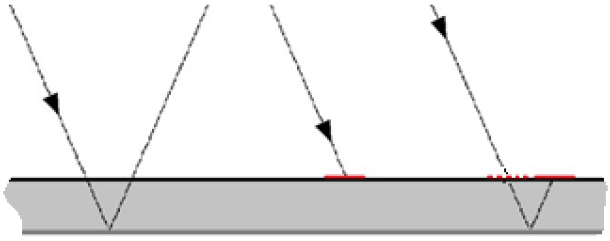

Fig. 16: Three solar ray paths and blocking mechanisms, a) ray is reflected on the rear surface of the mirror, beam is not obstructed, b) deposited particle blocks solar ray at entrance into the mirror and c) solar ray is reflected, however, it is blocked after exit of the mirror body. Source: author

Furthermore, at the beginning of a cleaning period (after cleaning), low soiling load tends towards secondary blocking. Later in the soiling period when more particles cover the surface, primary blocking is becomes dominant. In addition, particle size [65] interferes with reflectance, due to the mass distribution within a particle set. Relatively speaking, a higher mass fraction is stored in the vertical axis in the case of larger particles, which influences the MDD, however they have less influence [66] on surface coverage. The project did not take the above effects into consideration.

4.2 Data Acquisition

The particle distribution was simulated with a simple numerical program (BASIC language). A soiling area of 1,000 x 1,000 area elements of the average particle diameter ($D_{[3,2]}$: 15.6um) were used. For total coverage at higher soiling load, a squared particle and area element shape was used. This condition was achieved with $5x10^6$particles randomly distributed.

The numerical simulation recorded the amount of primary covered area elements and secondary covered area elements (according to the physics of reflectance) and the edge effect ignored (continuity of model).

WP 2 of the project repeated the methods described in WP 1 (chapter 2), however soiling material from Almeria (Submission one) was added to the experiments.

For the experimental work, one additional soiling material from Almeria PSA was used. The material was taken from the ground and prepared (by drying and sieving) identically as for the Silt-Material. The particle size was measured by a laser diffractometer (Malvern, MasterSizer 3000).

4.3 Experimental Results

Figure 17 shows a representative soiling load (MDD) versus reflectance (RSe) diagram. Additionally, a higher soiling load (MDD: > 2.5g/m^2) was conducted. This shows visible exponential non-linear behaviour between reflectance and MDD.

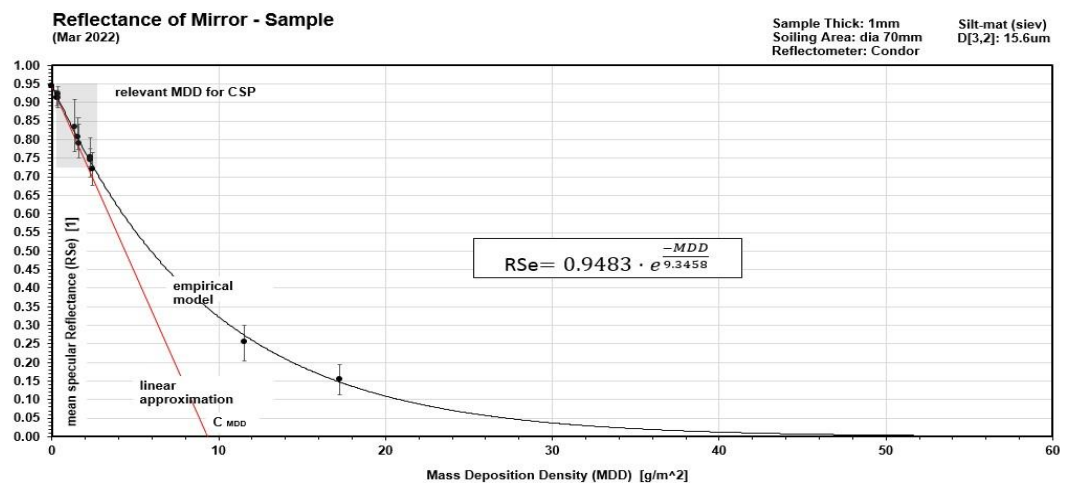

Note: Grey area is for CSP relevant range

Fig. 17: Diagram shows a representative MDD vs RSe diagram with empirical model and initial tangent with C_{MDD}.

In opposition to the commonly assumed linear behaviour, the MDD versus RSe correlation is exponential and described mathematically modelled as follows:

$$RSe_{(MDD)} = RSe_{\max} \cdot e^{\frac{-MDD}{C_{MDD}}} \qquad \text{Eqn. 4-2}$$

Maximum specular reflectance (RSe_{max}) is 0.945[1] (measured value) and the exponential constant (C_{MDD}) retrieved by exponential correlation are shown in Table 3.

Lower C_{MDD} values at smaller particle sizes highlight the capability to cover the surface at a lower mass deposition density.

Table 3: Summary of the parameters used for the soiling model

Material Grade:	**Size class:**	**De Brouckere Diameter:** ($D_{[4,3]}$), [μm]	**Sauter Diameter:** ($D_{[3,2]}$), [μm]	**C_{MDD}:** [g/m²]
Silt-mat.	Course	39.0	18.2	22.7273
	Ground	27.8	15.6	9.3458
	Fine	13.7	7.0	8.8496
Almeria-mat	Course	39.5	19.2	19.2308
	Ground	27.7	15.6	9.2593
	Fine	14.4	7.5	8.0645

Coverage ratio (q) was measured using a digital microscope on several soiled mirror samples. Five micrographs of each mirror sample were analysed with imaging processing software (ImageJ), which provided the coverage ratio. Figure 18 shows a representative diagram of q versus MDD plot, where five samples per target MDD were analysed and averaged. The coverage ratio also does not follow the soiling load linearly as described in Fig. 17.

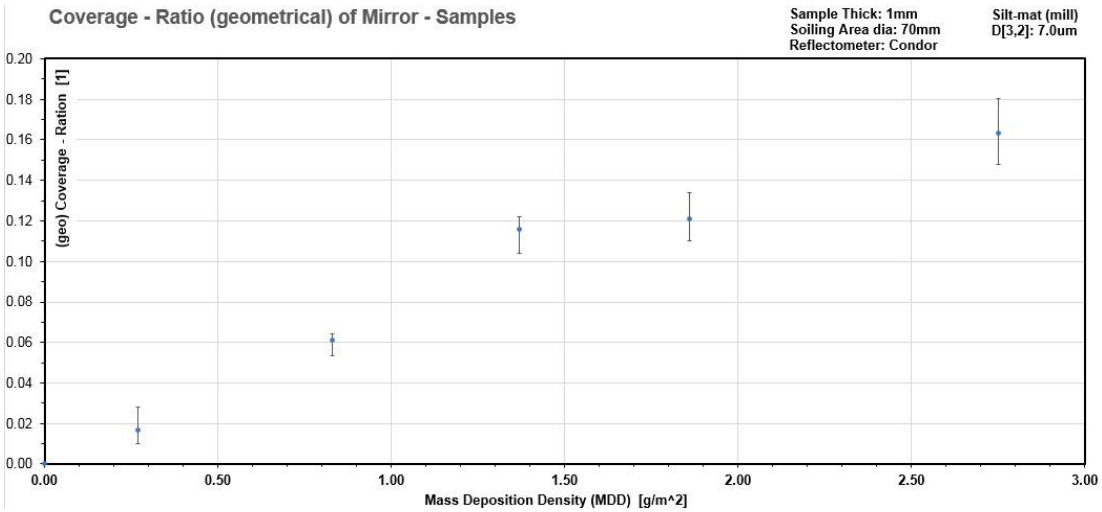

Fig. 18: A representative diagram of geometrical coverage ratio versus MDD graph with error bars.

4.4 Simulated Coverage and empirical Coverage Model

The simulated data was processed (normalized) and plotted against the two-parameter coverage ratio, geometric coverage ratio (q_{geo}) which represents the measured value when the effective coverage ratio (q_{eff}) appears when secondary blocking is also taking into consideration. Both exponential constants were calibrated to real measured values at the position $\left(n_{part}^{NORM}\right)$ = 1.

Equation 4-3 a, b highlights both empirical models with the optimized exponential constants (C_{geo}^{OPT} = 0.9423 and C_{eff}^{OPT} = 0.4705).

$$q_{geo} = q_{\max} - e^{-\frac{n_{part}^{NORM}}{0.9423}} \qquad \text{Eqn. 4-3a} \qquad \text{and}$$

$$q_{eff} = q_{\max} - e^{-\frac{n_{part}^{NORM}}{0.4705}} \qquad \text{Eqn. 4-3b}$$

Figure 19 shows normalized deposited particle $\left(n_{part}^{NORM}\right)$ versus both coverage ratios (q_{geo} red and q_{eff} black). The q_{eff} (black) has a higher gradient than the q_{geo}, which indicates more pronounced coverage behaviour (primary and secondary blocking).

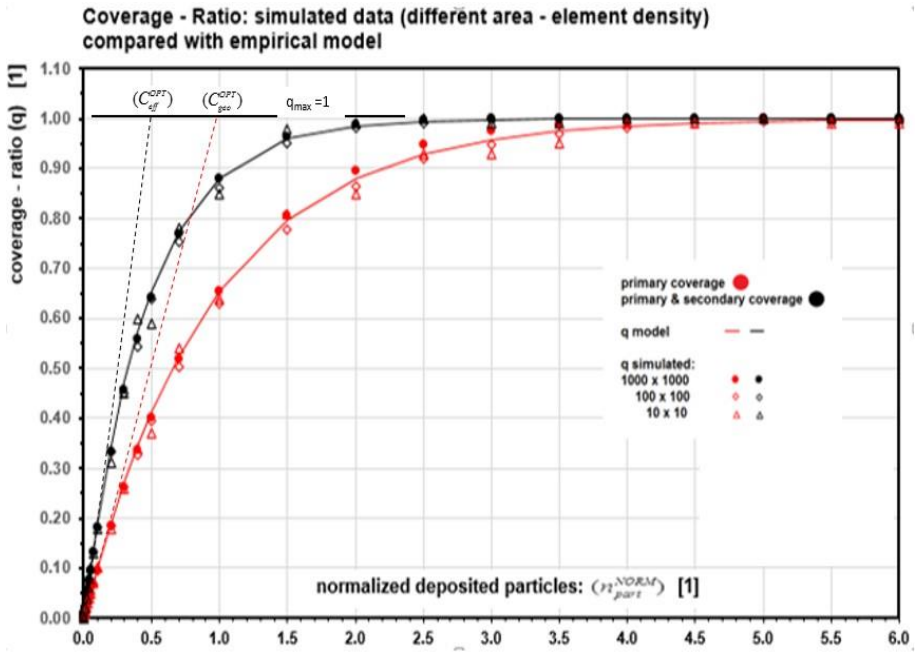

Fig. 19: Diagram shows simulated coverage ratio results of three different area element densities. Optimized empirical model is created from 1,000 x 1,000 area elements.

4.5 Coverage Ratio Model transferred to specular Reflectance Model

A comparison of both coverage ratio values (q_{geo} and q_{eff}) (Submission three) with experimental values and the assumption of the direct influence of deposited particle on specular reflectance was used to formulate a coverage ratio versus specular reflectance model. The model assumed that the boundary condition "clean" (uncovered soiling area) has the highest specular reflectance (RSe_{max} = 0.945[1]) and a totally covered soiling area has no specular reflectance (RSe = 0).

The empirical model which uses q_{eff} has a much more consistent correlation with the measured data, and therefore the following mathematical equation was persuade.

$$RSe^{eff}_{\left(n^{NORM}_{part}\right)} = RSe_{\max} \cdot e^{\left(-\frac{n^{NORM}_{part}}{C^{OPT}_{eff}}\right)} \qquad \text{Eqn. 4-4}$$

Figure 20 illustrates normalized deposited particles $\left(n_{part}^{NORM}\right)$ versus specular reflectance (model) (RSe_{eff}) and coverage ratios (model) geo and eff.

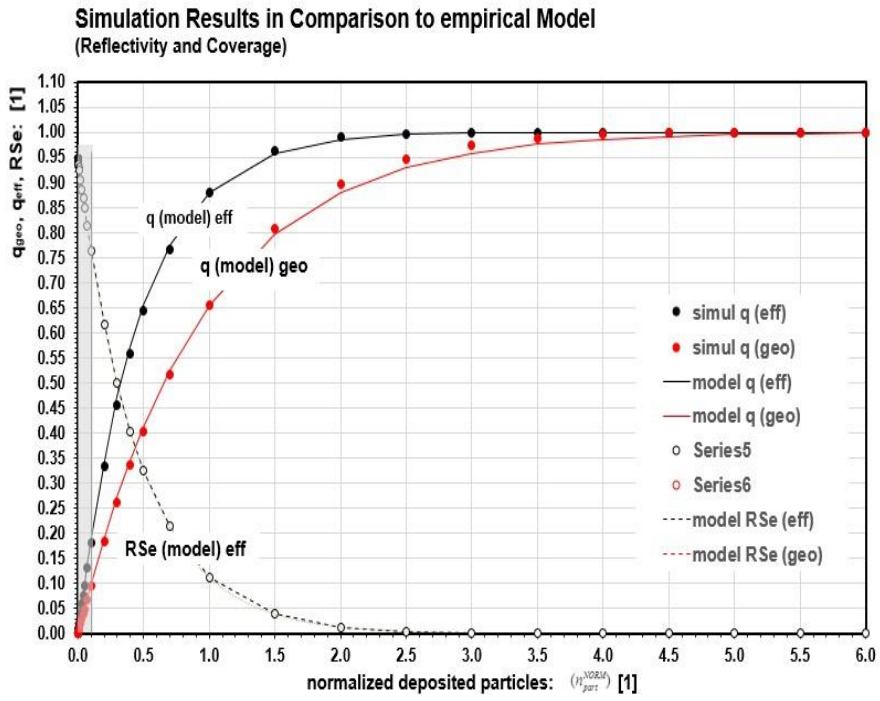

Fig. 20: Diagram shows simulated (optimized) results of coverage ratio and reflectance in dependency of deposed particles in comparison with their individual empirical model.

Note: Normalized deposed particles range is < 0.1[1]. **Note:** Grey area is for CSP relevant range

Furthermore, the measurable soiling load parameter (g_{geo} and MDD) were integrated in the specular reflectance model. Specular reflectance (RSe_{eff}) versus geometrical coverage ratio (q_{geo}) model:

Eqn. 4-3a in Eqn. 4-4:

$$RSe^{eff}_{(q_{geo})} = RSe_{\max} \cdot e^{\frac{C_{geo}^{OPT}}{C_{eff}^{OPT}} \cdot \ln\left(q_{\max} - q_{geo}\right)} \qquad q_{max} = 1 \qquad \text{Eqn. 4-5}$$

Figure 21 highlights all $RSe_{(qgeo)}$ results correlated with the specular reflectance model (RSe). The empirical model follows the measured data acceptably. The error becomes larger at larger soiling loads.

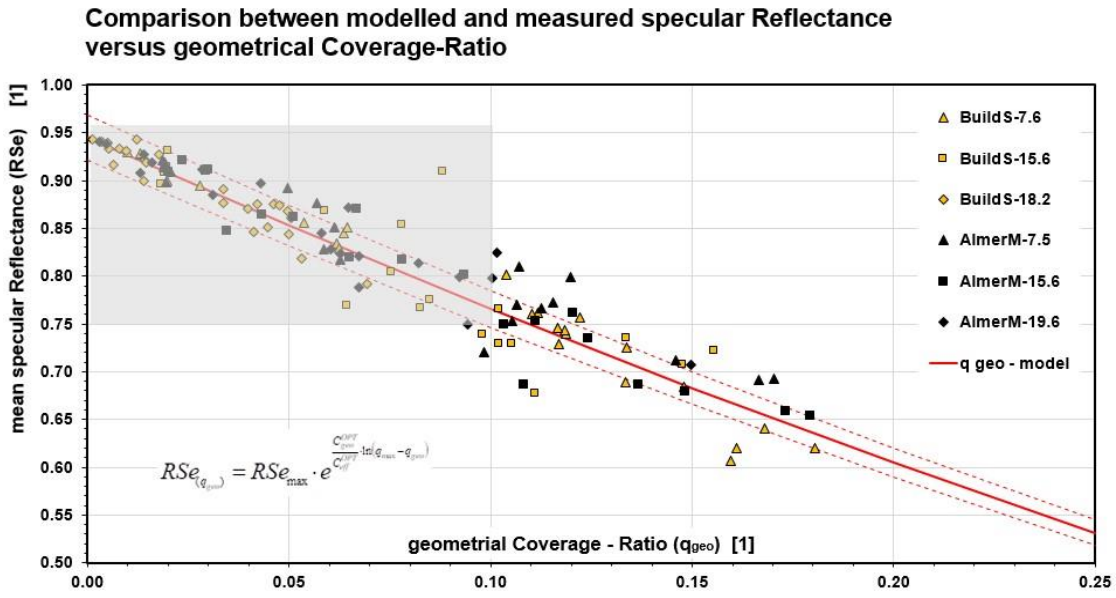

Note: Grey area is for CSP relevant range

Fig. 21: A comparison between modelled and measured specular reflectance and additionally provides a 5% area of the modelled data.

Specular Reflectance versus Mass Deposition Density Model

Furthermore, a MDD versus specular reflectance model was also formulated. The known values (The lower boundary is defined as MDD = 0 and RSe_{max} where the upper boundary is defined as MDD = C_{MDD} and RSe = 0) were proportionally fitted. For simplicity, a linear model is created.

$$MDD_{\left(n_{part}^{NORM}\right)} = n_{part}^{NORM} \cdot \frac{C_{MDD}}{C_{eff}^{OPT}} \qquad \text{Eqn. 4-6}$$

Figure 22 highlights the calibrated MDD results with its measured MDD data. Comparison between the measured MDD and “calibrated” MDD model provides a consistence correlation.

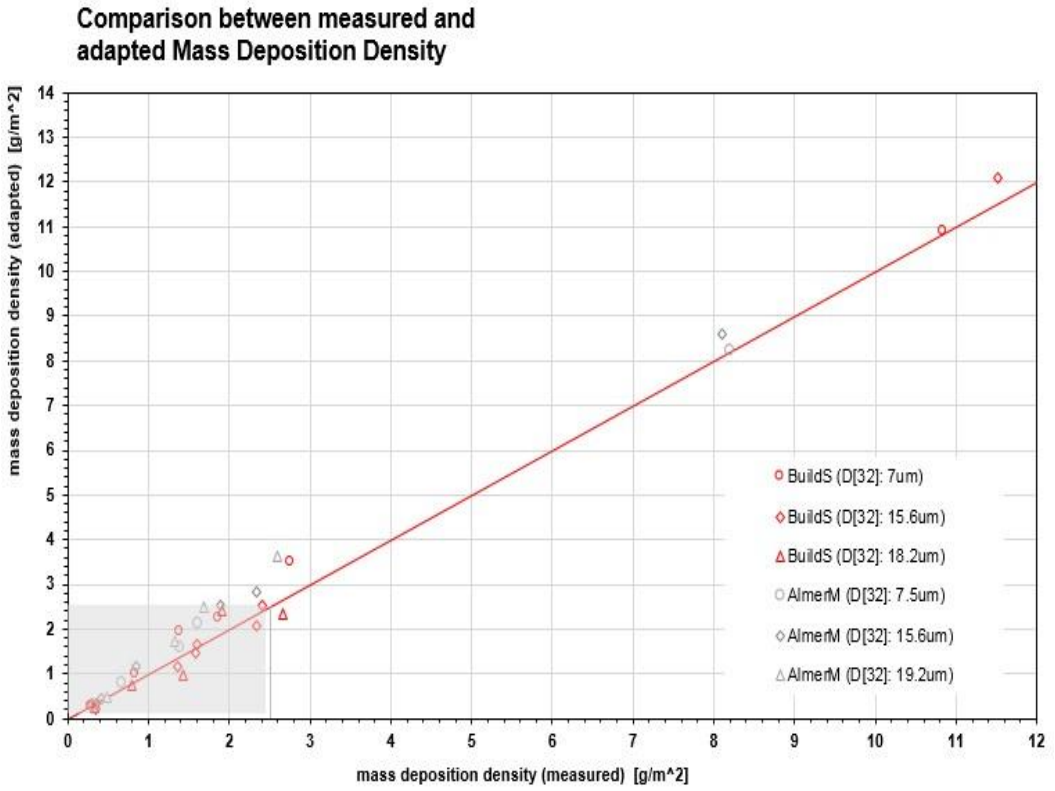

Note: Grey area is for CSP relevant range

Fig. 22: Comparison between measured MDD data and MDD data adapted to C_{MDD} parameter.

4.6 Comparison of linear and exponential (basis) Reflectance Model

The linear approximations are practical for use but have marked differences to the real specular reflectance values. A comparison of a linear correlations with the exponential model revealed at that relatively higher soiling load (MDD) values the difference becomes significant.

Figure 23 shows the two models (linear model) and exponential model. A comparison between the commonly used linear model (linear correlation, grey line) and the exponential model (black line) was carried out on the example of two reflectance thresholds (0.9[1] and 0.8[1]). The analysis estimates the potential yearly cleaning cycles reduction on the daily soiling load assumption of ($0.1 g/m^2$).

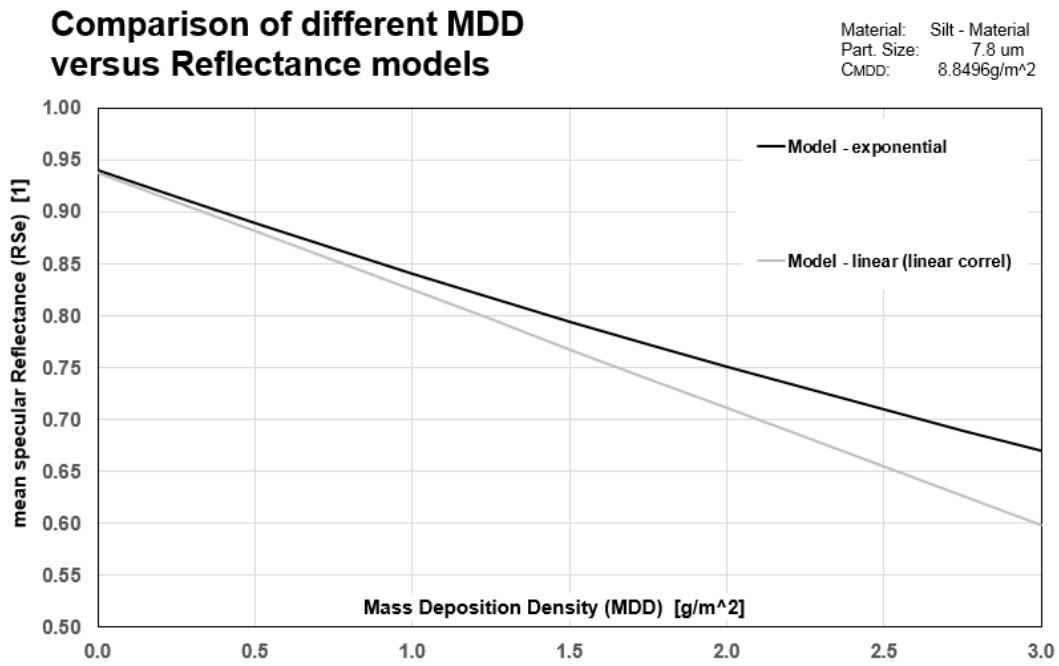

Fig. 23: Comparison of the two linear models and the exponential model.

Table 4 highlights the absolute yearly cleaning effort of both soiling models, and the absolute and relative differences.

Table 4: Comparison between the exponential soiling model with the linear soiling model, in terms of annual cleaning cycles, at two reflectance thresholds (RSe 0.9[1] and 0.8[1]).

	RSe: 0.9[1]						
Soiling–material	**MDD (exp)**	**MDD (linear)**	**Difference of MDD**	**Yearly runs (exp)**	**Yearly runs (linear)**	**Yearly diff run**	**relative reduction**
	[g/m^2]	[g/m^2]	[g/m^2]	[1]	[1]	[1]	[%]
(1)	(2)	(3)	(4)	(5)	(6)	(7)	(8)
SiltM-7.8	0.39	0.33	0.06	93.4	109.9	16.4	15.0
SiltM-15.6 (*)	0.41	0.45	-0.04	89.4	81.1	-8.2	-10.1
SiltM-18.2	1.02	0.96	0.07	35.6	38.0	2.5	6.5
AlmerM-7.5	0.36	0.34	0.02	100.1	107.1	7.0	6.6
AlmerM-15.6	0.41	0.32	0.09	89.3	114.4	25.1	22.0
AlmerM-19.2	0.85	0.71	0.14	43.0	51.4	8.3	16.3

Note: Exponential (exp)

	RSe: 0.8[1]						
Soiling–material	**MDD (exp)**	**MDD (linear)**	**Difference of MDD**	**Yearly runs (exp)**	**Yearly runs (linear)**	**Yearly diff run**	**relative reduction**
	[g/m^2]	[g/m^2]	[g/m^2]	[1]	[1]	[1]	[%]
(1)	(2)	(3)	(4)	(5)	(6)	(7)	(8)
SiltM-7.8	1.43	1.21	0.22	25.4	30.0	4.5	15.2
SiltM-15.6 (*)	1.5	1.53	-0.03	24.3	23.8	0.5	-2.2
SiltM-18.2	3.76	2.99	0.78	9.7	12.2	2.5	20.6
AlmerM-7.5	1.34	1.09	0.24	27.2	33.3	6.1	18.2
AlmerM-15.6	1.5	1.21	0.28	24.3	30.0	5.7	19.0
AlmerM-19.2	3.11	2.29	0.82	11.7	15.9	4.2	26.4

Note: (4): The difference of MDD represents the real MDD (at 2g/m^2) to the with the linear model calculated MDD (at 2g/m^2)
Note (*): in one case the linear model provided higher values and therefore better results than exponential model.
Note: Exponential (exp)

The results are not consistent, in particular, the negative results of silt material (15.6μm), however it is assumed that this is a result of difficulties in the test rig handling, rather than fundamental differences in the soiling process. The potential reduction of cleaning effort (cycles), when using the exponential model rather than a linear model, is in the range of approximately 5-25%, dependent on soiling material and average particle size.

4.6.1 Soiling Element Parameter-based Soiling Model

The project developed based on analysis of specific soiling parameters, which describes an individual soiling process, a reflectance model. Such an analytical model can potentially calculate reflectance based on measured data. From the experiment, the C_{MDD} constant express the overall soiling process, specific material properties of the deposited soiling material are not expressed. This project extracted further parameters from the C_{MDD}, average particle size ($D_{[4,3]}$) and particle density (ρ_{part}), detailed in Submission two.

The effect of C_{MDD} provided be a different mass distribution on a particle of variable size, however other parameters, such as density also play a role. It is assumed that further parameters, related to one specific soiling process could enhance this soiling model, however these were not integrated in the model.

This approach of development, uses the volume based De Brouckere particle diameter ($D_{[4,3]}$). The further analysis used particle mass values and therefore the volume based diameter data provides better data when processing volume dependant density data. Furthermore, the particle density parameter (ρ_{part}) is used due to the better bulk material description, Submission two, see Table 7.

Enhanced Soiling Model

The shape of a particle is assumed to be a sphere. Therefore, the total mass of soiled particles are

$$m_{part}^{soiled} = \left(n_{part}^{NORM} \cdot N_{a-ele}\right) \cdot \left(\frac{\pi}{6} \cdot D_{[4,3]}^{3}\right) \cdot \rho_{part} \qquad \text{Eqn. 4-7}$$

Where total soiled mass (m_{part}^{soiled}, unit kg), amount (normalized) of simulated particles (n_{part}^{NORM}), amount of area elements in the simulation (N_{a-ele}, 1,000,000) and particle density (ρ_{part}, unit kg/m^3).

Verticle projected area is related to the diameter of the particle:

$$a_{part}^{soiling} = \left(\sqrt{N_{a-ele}} \cdot D_{[4,3]}\right)^2 \qquad \text{Eqn. 4-8}$$

Where $a_{part}^{soiling}$ is the total simulated soiling area, not the area of one soiling element.

MDD model Eqn. 4-7 and Eqn. 4-8:

$$MDD = \frac{\left(n_{part}^{NORM} \cdot N_{a-ele}\right) \cdot \left(\frac{\pi}{6} \cdot D_{[4,3]}^3\right) \cdot \rho_{part}}{N_{a-ele} \cdot D_{[4,3]}^2} = \left(n_{part}^{NORM}\right) \cdot \left(\frac{\pi}{6} \cdot D_{[4,3]}\right) \cdot \rho_{part} \qquad \text{Eqn. 4-9}$$

The normalized amount of distributed particles:

$$n_{part}^{NORM} = \frac{6 \cdot MDD}{\pi \cdot D_{[4,3]} \cdot \rho_{part}} \qquad \text{Eqn. 4-10}$$

From the average specular reflectance model Eqn. 4-2 and Eqn. 4-4:

a) $RSe = RSe_{\max} \cdot e^{-\frac{MDD}{C_{MDD}}}$ and b) $RSe = RSe_{\max} \cdot e^{-\frac{n_{part}^{NORM}}{C_{eff}^{OPT}}}$

The exponent can be expressed as:

$$\frac{MDD}{C_{MDD}} = \frac{n_{part}^{NORM}}{C_{eff}^{OPT}} = \frac{6 \cdot MDD}{\pi \cdot D_{[4,3]} \cdot \rho_{part} \cdot C_{eff}^{OPT}} \qquad \text{Eqn. 4-11a}$$

and the C_{MDD}:

$$C_{MDD} = \frac{\pi \cdot D_{[4,3]} \cdot \rho_{part} \cdot C_{eff}^{OPT}}{6} \qquad \text{Eqn. 4-11b}$$

and introduced in the average specular reflectance model Eqn. 4-2:

$$RSe = RSe_{\max} \cdot e^{-\frac{6 \cdot MDD}{\pi \cdot D_{[4,3]} \cdot \rho_{part} \cdot C_{eff}^{OPT}}} \qquad \text{Eqn. 4-12}$$

Particle density values (Submission four), will be too low when taking the analysing process into consideration and it can be assumed that silica's material density will overestimate the real specular reflectivity. Figure 24 plots the calculated average specular reflectance model (Eqn. 4-12) data using both density data (measured and silica density) with the experimental reflectance data.

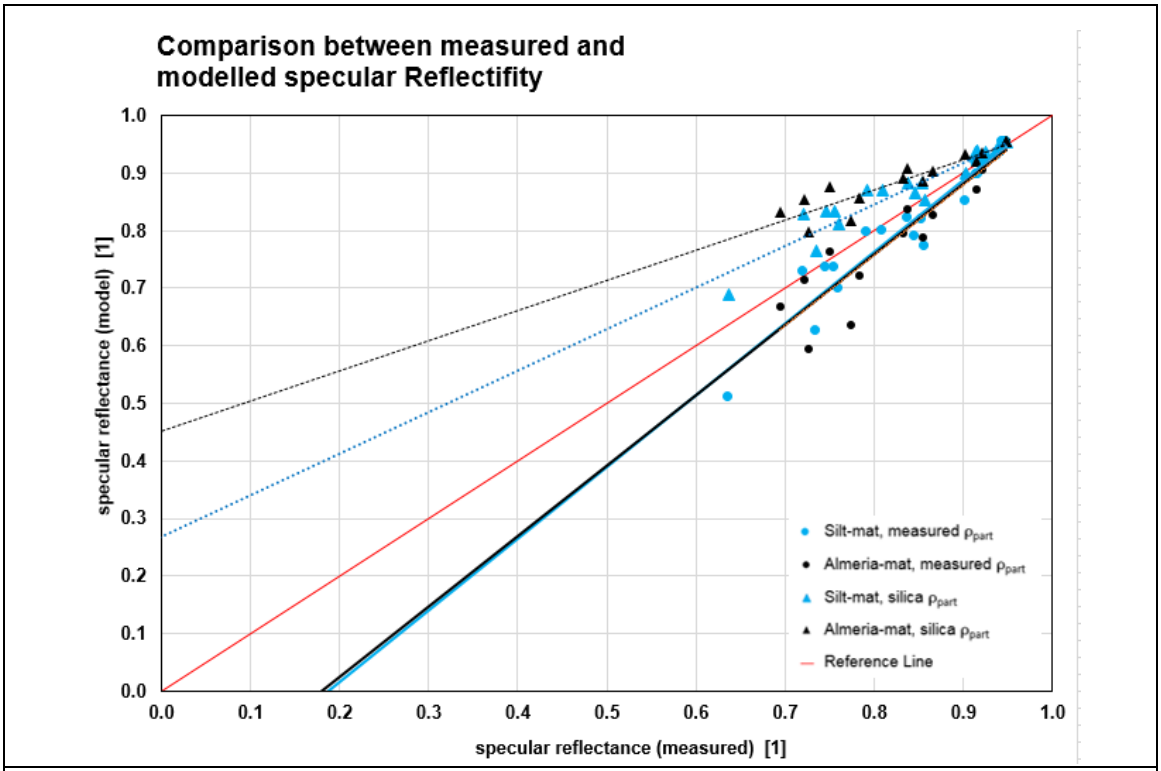

Fig. 24: Comparison of measured reflectance data with the particle size integrated specular reflectance model. The relevant reflectance range: RSe >0.75[1].

All particle density values and the results of the linear correlation can be seen in Table 5.

Table 5: All specular reflectance comparison results and the relative error.

Soiling-Material:	**Density part**: [kg/m^3]	**Gradient:** [1]	**relative error:** [%]
Silt-material	1,303.9	1.2452	24.4%
Almeria-Mat	955.7	1.2227	22.3%
Silt-material	2,500	0.7221	27.8%
Almeria-Mat	2,500	0.5252	47.48%

As expected the reflectance model, dependent on the particle density value used, either overestimates or underestimate the measured reflectance data. The gradient of the linear fit compared with the ideal gradient reveals a relative error of up to 47.5%, when most relative errors are less than 30%.

An additional effort to improve particle density data assumed that the final and most representative density value is still too small. A mathematical correlation (power function) was used by extrapolation and analysing the gradient numerically (threshold 0.01% from previous value) to determine a particle density value closer to the real value. It is assumed that this more practical method can be optimized for future use.

When the following equation represents the mathematical correlation (power function):

$$\rho_{part} = a \cdot sequ^{b} \qquad \text{Eqn. 4-13}$$

The parameter (sequ) represents one measurement sequence.

Table 6 highlights the parameter of the mathematical correlation, the chosen sequence and the optimized particle density value.

Table 6: All results occurred during the optimisation process of the particle density.

Soiling-Mat:	**Parameter**: (Eqn. 4-13)	**Sequ (*)** [1]	ρ_{part} (*) [kg/m^3]
Silt-Mat	a: 1087.8 b: 0.0615	615.5	1,402.1
Almeria-Mat:	a: 643.69 b: 0.1457	1457.5	1,330.9

Note: (*) Optimized particle density value.

Table 7 shows the model quality with the optimized particle density values.

Table 7: Model with optimized particle density.

Soiling-Material:	**Density part:** [kg/m³]	**Gradient:** [1]	**Relative error:** [%]
Silt-material	1,402.1	1.1755	17.5%
Almeria-Mat	1,330.9	0.9254	7.4%

The exponential reflectance model with integrated soiling process data, in particular the enhanced particle density, provides a tool to forecast solar collector performance on the basis soiling material data to a relative error of < 20%. Even on higher soiling loads this empirical model provides suitable reflectance values. Furthermore, the integration of particle parameter into the model makes it more useful in the analysis of a specific soiling process, for example solar field validation.

However, further particle characteristics or weather parameter could potentially improve and expand this specular reflectance model.

5 Adhesion Force Analysis

Adhesion forces between particle and particle and between particle and mirror surface are the major effects which govern the soiling in CSP. They have the potential to optimize solar energy operations (this includes photovoltaic and evacuated tube collectors). The soiling process in solar energy industry, is not complete understood, not on the macroscopic level [67]. Reference [67] highlights that no standard or recommendation exists which deals with this issue.

A method to simulate natural soiling, which includes sequential soiling as well as condensation was developed. Finally, from literature, the centrifuge device was chosen to simulate the removal force for particles on mirror samples. The relative difference of geometrical coverage ratio was used as a parameter to quantively assess different soiling loads (MDD), which were applied with multiple methods.

This WP includes the condensation process, which occurs every night to some extent on a solar field. The water film created generates effects known as particle caking and capillary aging. This affects moving particles according of their size and mass, and in addition, enlarges the contact area between the particles and surface (between particles). These additional effects increase the adhesion forces and therefore need to be included in soiling experiments. Due to complexity a further soiling effect, cementation, was not part of these experiments, even it potentially adds to the adhesion forces.

From literature [68] single soiling sequences with condensation are known. However, the constant condensation and therefore interference with particle constellation to each could have and amplifying effect on the adhesion forces. The investigation into an appropriate test sequence, test method for adhesion force and proving the differences between single and multiple soiling (in connection with condensation) are the main objectives of this WP.

5.1 Removal Force in the context of Adhesion Force

The experimental analysis of a force is executed by adding a controllable and measurable force, which acts in an opposite direction. The reaction of the object to the applied force can be measured and thus provide a quantitative result. In the case of adhesion force of particles an external force is applied (removal force), which is controlled (force magnitude is known) and has the potential to move (remove) the particles.

Even literature can explain the adhesion forces between individual particles and surface, so it impossible to describe the adhesion effects of bulk material due to

its complexity [69, 70]. Therefore, a macroscopic effect was chosen as an output parameter, the difference of the geometrical coverage ratio [67, 69].

From literature, several methods are known for experimental applications, which apply removal forces on particles (Submission five). These are commonly the Atomic Force Microscope (AFM), Vibration method, Fluid-Dynamic (air flow) method, Impact method and recently Surface Free-Energy method [71, 72, 73, 74]. While the AFM in known for its time-consuming sample preparation and non-robust process, the Vibration method applies its force vertically, and the Fluid Dynamic (air knife) process lacks in accuracy [67]. A similar issue applies to has the Surface Free Energy method, the sample preparation is a time demanding and finally, the results provide an estimation of the expected adhesion forces of a specific particle-glass pair [74]. Due to the use of thin (thickness: 1mm) mirror samples and the experimental effort of the impact test was also rejected. Therefore, this project chose the centrifuge method, [67, 71, 75] because of it practicality and availability. The removing force (drag from airflow) has a horizontal direction (natural wind) and the removed particles leave the mirror surface. Figure 25 shows an illustration of the several methods of analysing adhesion forces of particles, described.

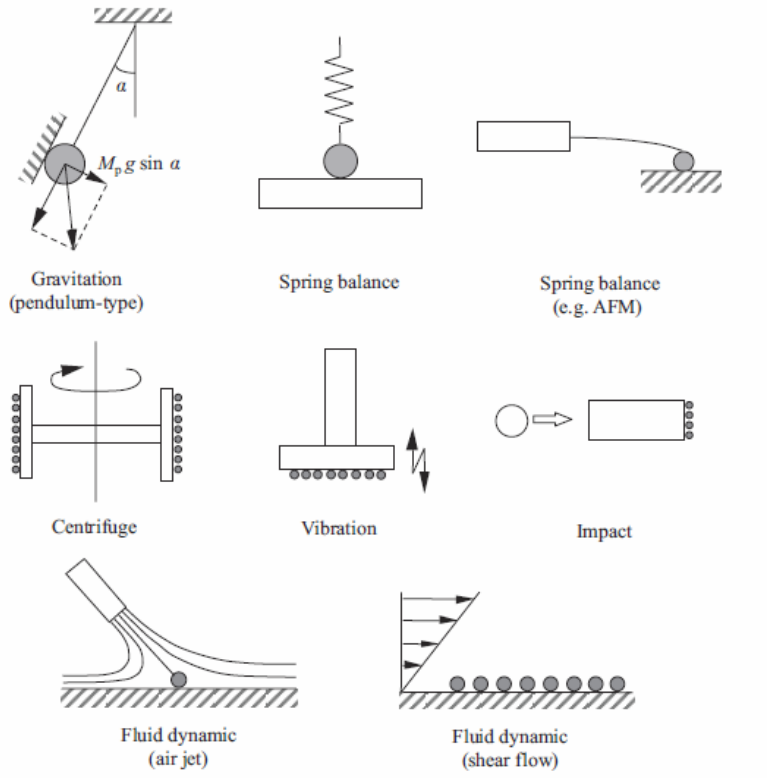

Fig. 25: Illustration of common methods to measure adhesion force of particles on flat surfaces.

Source: [71, 72]

The Centrifuge Method rotates a soiled mirror sample, which is located on a table. The rotation generates an inwards (rotation centre) acting centripetal force [76, 75], which acts in a horizontal direction. The removal force is the sum of radial force (negative centripetal force) and tangential force (drag force) and can be calculated as follow:

Radial direction:

$$F_{cent} = \frac{m \cdot V^2}{r} \qquad \text{Eqn. 5-1}$$

where:	Force in radial direction:	(F_{cent})	N
	Mass of object:	(m)	kg
	Velocity:	(V)	m/s
	Distance from centre:	(r)	m

Tangential direction:

$$F_{drag} = 8 \cdot \rho_{air} \cdot d_{part}^2 \cdot u_8^2 \qquad \text{Eqn. 5-2}$$

where:	Drag force:	(F_{drag})	N
	Density of air:	(ρ_{air})	kg/m3
	Particle diameter:	(d_{part})	m
	Friction/shear velocity	(u_s)	m/s

For these equations, force in normal direction is mainly the lift force and the particle adhesion forces (Van der Waals forces, capillary forces and gravitational force, Submission two).

Normal Direction:

$$F_{lift} = \frac{0.744 \cdot \rho_{air} \cdot d_{part}^4 \cdot u_8^4}{\nu^2} \qquad \text{Eqn. 5-3}$$

Figure 26 illustrates the main forces acting on the centrifuge experiment [77]. Resuspension (Submission two) is initiated by a particle gliding over the mirror surface, than the particle begin to roll and finally leave the mirror surface (lift).

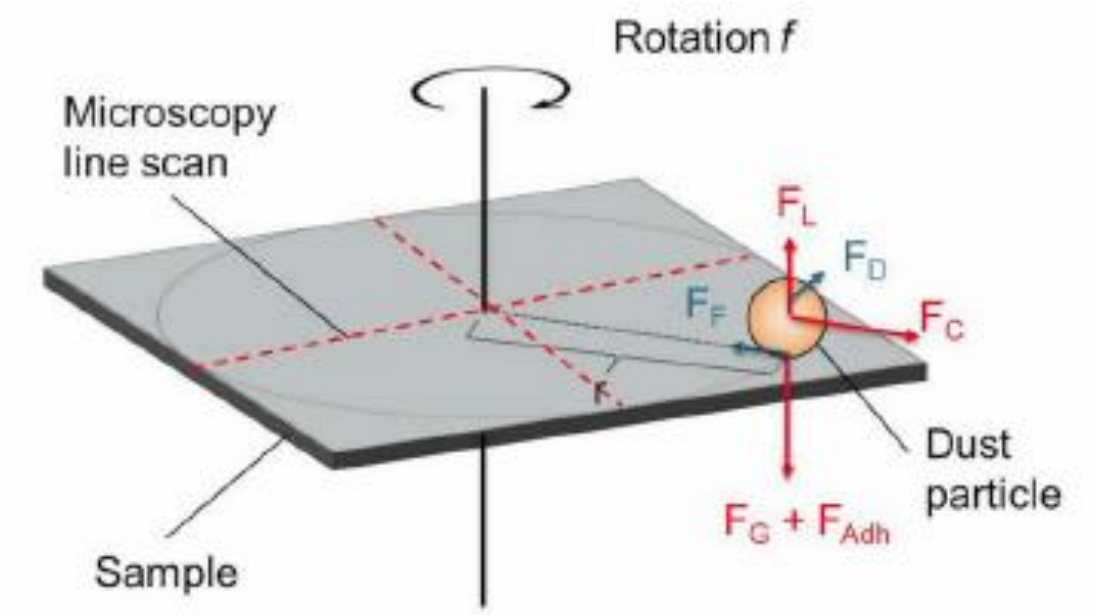

Fig. 26: Illustration of the main forces acting on a spherical particle during the centrifuge test, to measure the horizontal removal forces. Source: [77]

It is expected that during the experiment particles will roll over the sample edge [76]. The threshold of gliding can be expressed as follows [76]:

$$F_{drag} + F_{lift} - F_{grav} > F_{adh} \qquad \text{Eqn. 5-4}$$

where:	Drag force:	(F_{drag})	N
	Lift force:	(F_{lift})	N
	Gravitation force:	(F_{grav})	N
	Adhesion force:	(F_{adh})	N

When [68] describes the critical condition for sliding as:

$$\left|F_{cent} + F_{draft}\right| > \left|F_{grav} + F_{adh} - F_{lift}\right| \qquad \text{Eqn. 5-5}$$

Note: Static friction k is assumed 1 (glass to glass surfaces) and therefore ignored [77].

The project used a centrifuge (spin coater) with a permitted revolution of 4,000rpm, however with applying special safety measures, a final test series with 6,000rpm was conducted. For comparison [68, 76] used 6,000rpm also when Reference [75] had a capacity of 15,000rpm.

Methodology

For the following experiments, condensation was applied to the soiled mirror sample in a dry lab chamber, in a defined ambient condition. Afterwards the adhesion effect introduced was analysed with the centrifugal method.

Material

The experiments were conducted as previously, with two soiling materials (Silt material and Almeria material, Submission two) of average particle size (De Brouckere particle diameter) $D_{[4,3]}$) 27.8μm and 27.7μm respectively. Also uncoated solar mirror samples (100 x 100mm, thickness: 1mm, Submission two). All samples were analysed comparing the geometrical coverage ratio differences from before, during and after the test sequences. Ambient conditions, temperature and relative humidity were measured.

Test Equipment

The lab ambient condition were constantly monitored and were follows:

Ambient temperature:	24°C	+/- 3°C
Relative Humidity:	49%	+/- 4%

The soiling experiments were all carried out with an artificial soiling test rig developed within this project, (Submission two). The condensation process was conducted on a laboratory dry chamber and a cooling plate Fig. 27a. The draft free dry chamber, ensured a place for a cooling plate, driven by a chiller device, suitable for temperatures below 10°C. The chiller provides deionized water at a

certain temperature to a meander through formed copper tubes within the cooling plate, under the actual cooling plate (cooper sheet). The ambient conditions within the dry chamber could be adjusted between 50-90% relative humidity (two humidifier) and temperature between 20–90°C, which was monitored constantly. The surface temperature of the cooling plate (lower surface of the mirror samples) was also monitored separately with an extra thermometer and flat temperature sensor Fig. 27b.

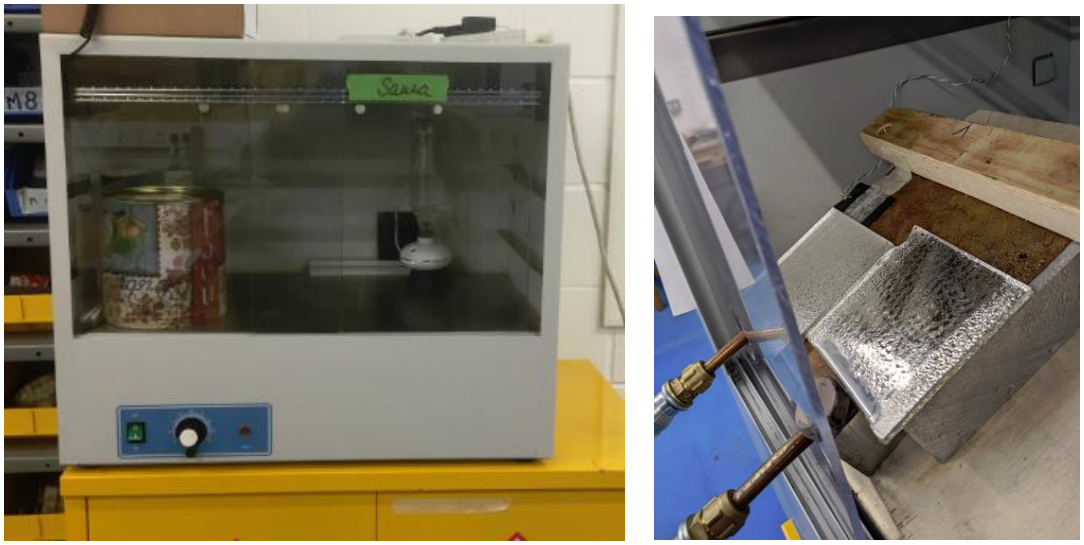

(a) (b)

Fig. 27: Photos of the (a) dry camber and (b) the cooling plate with mirror sample and on the rear edge additional thermometer visible.

Experimental Method and Procedure

The natural soiling process was simulated, including repeated soiling and condensation. Such a soiling test simulates a maximum cleaning cycle, with a final specular reflectance of ~75% in 10days (Submission one). Four soiling runs each MDD 0.5g/m^2 and a final soiling load MDD 2.5g/m^2 were conducted (MDD: 1.5g/m^2 was not carried out). A condensation phase was carried out between each soiling run, with a duration of 20min (replicates 2–3h condensation every night) [77]. Further soiling was only accomplished with absolutely dry mirror samples (drying period ~ 5h). The conditions in the dry chamber were on the basis of a real situation reported in reference [57], where a temperature difference of approximately of 5.1K between upper and lower mirror surface was measured. A pre-test series highlighted this is the transition between invisible and visible

condensation on the upper mirror surface, Submission five. Ambient temperature in dry camber was between 20°C and 23°C.

Several soiling test series were carried out to study the differences of the results compared between the three soiling test series. One test series (REAL) was carried out with sequential soiling and condensation as descript above, when a second test series (DRY) repeated the test series REAL however without condensation. Test series REFERENCE reached the final soiling load in one soiling process and with an expanding condensation duration. Figure 28 highlights the test series pattern of all the test series.

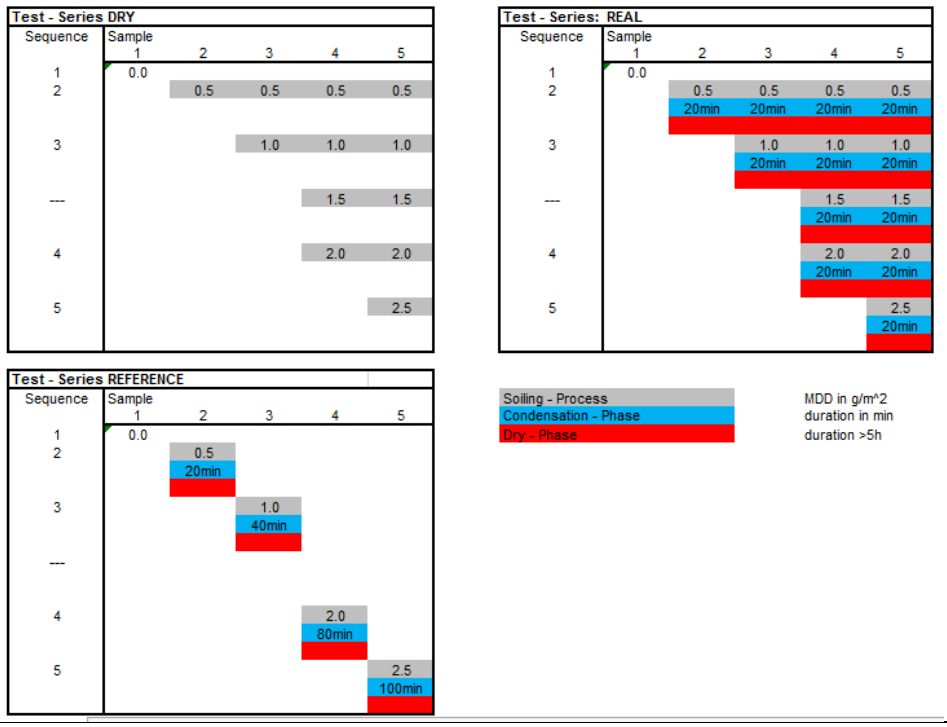

Fig. 28: Illustrations of the three different pattern of test sequences, carried out during the experimental work.

In order to simulate removal force, parallel to the mirror sample surface, a centrifuge device (Co. Electronic Micro Systems) was used, which usually is used to coat wafer samples. Revolutions of up to 6,000rpm were possible, however 4,000rpm was used for safety reasons. In the final experiments 6,000rpm were used with a very long duration of acceleration phase, which allowed the operator to move to a safe location. A repeatedly correct position

was achieved using two hair crosses fixed on a thick (20mm) plastic glass plate. The duration of spinning (final revolution) was 60s, the duration does not influence the results [57].

Figure 29 shows the centrifuge in total and detailed with the mirror sample.

(a) (b)

Fig. 29: Photos of the centrifuge, (a) the centrifuge in total and (b) close up of the mirror sample in the centrifuge.

Table radius max:	30mm
Revolution max:	6,000rpm

The maximal adhesion force compared to capillary force max (Submission two) is significantly lower, however particle shape and surface condition is not taken into consideration. A revolution of 6,000rpm is sufficient according to Reference [57]. The soiling area of each mirror sample is circular and has a diameter of 70mm. The edge of the soiling area is not adequately soiled and therefore the outer edge is not analysed. The locations 5mm, 10mm, 20mm and 30mm (relative to the centre) were analysed.

Coverage Ratio for Analysis

The parameter coverage ratio (q, Submission two) is used to compare and analyse the likelihood of relocating a particle, with a particular removal force.

Micrographs (digital microscope, Submission two) were taken before and after the spinning procedure and analyse with imaging processing software (ImageJ, Submission two). The particles size or equivalent diameter, the amount of particles within each class were compared. A simple pattern to which the microscope was calibrated, ensured that the same location was analysed each time. The comparative parameter is the coverage ratio change in percentage.

Results

Figure 30 shows the averaged change in coverage ratio (Δq_{geo}) according the mass deposition density. In addition, it was expected that the influence of the three condensation regimes highlights significant differences in the reflectance outcome. The averaged reflectance results can be seen in Figure 30.

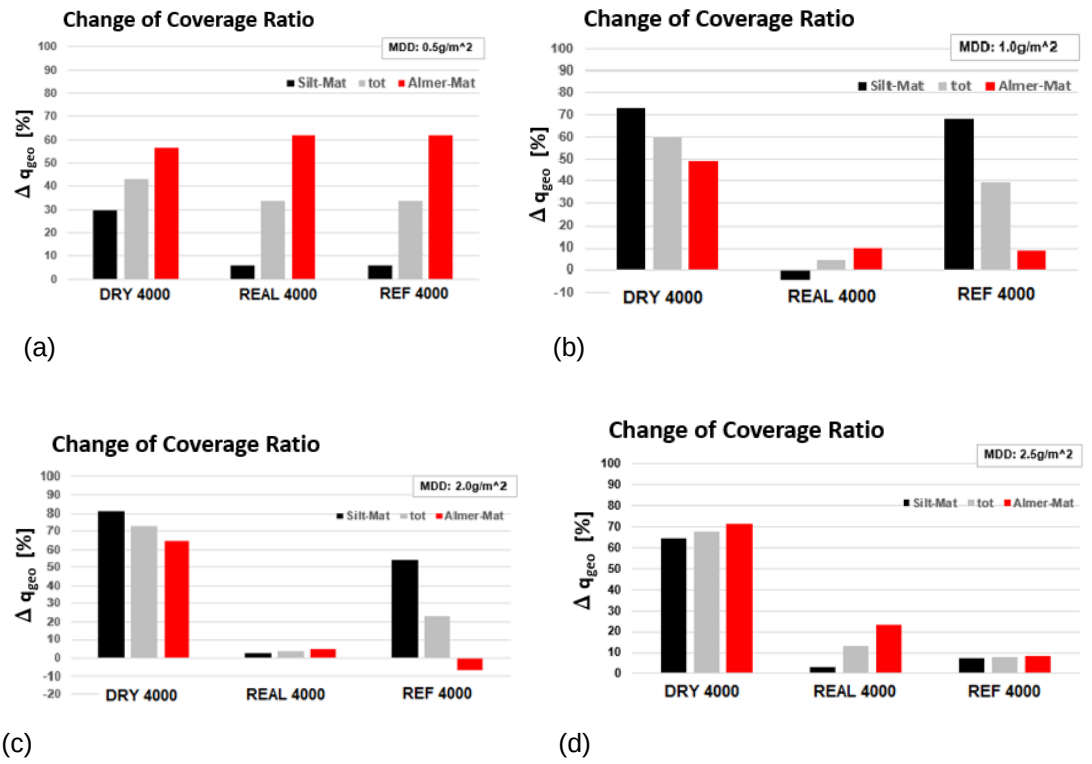

Note: REFERENCE Series is (REF)

Fig. 30: Diagram of the four condensation experiments, presented according to the different mass deposition density values, (a) 0.5g/m^2, (b) 1.0g/m^2,(c) 2.0g/m^2 and (d) 2.5g/m^2

The major result is that the results are not consistence, however all condensation groups have a distinguishing difference within a MDD series. In addition, differences between soiling materials (Silt material and Almeria Material) are visible, and it is assumed that these effects are based on particle shape, size and surface roughness.

The DRY series shows the biggest reduction of coverage ratio (Δq_{geo}), which can be explained by the absence of any particle caking and capillary aging effects. The results of the remaining condensation series (natural (REAL) condensation or one off (REFERENCE) is not conclusive. There is no difference at the low (MDD: 0.5g/m^2) case due to a constant condensation test regime, therefore the identical results would be expected.

It is not clear from the remaining soiling load results, which condensation regime produce bigger adhesion effect. However, as the last series (MDD = 2.5g/m^2) has a difference, this might be due to such problems as in experiment handling or an unexpected effect. The REFERENCE series shows a bigger reduction of RSe than the REAL series, which to some extent was expected.

A final test series with a 6,000rpm revolution became possible by implicating additional safety measures. This test series processed mirror samples with a soiling load of MDD = 2.5g/m^2 which assumingly provides the biggest difference in results and is therefore visible. Figure 31 shows the difference in coverage ratio (Δq_{geo}) of two different revolutions (4,000rpm and 6,000rpm) for the example of MDD = 2.5g/m^2.

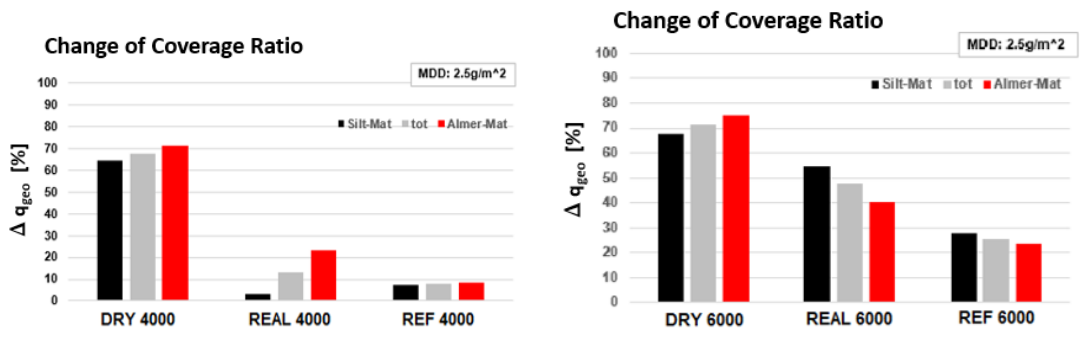

(a) (b)

Fig. 31: Diagram of the condensation experiments (MDD: 2.5g/m^2), experiments carried out with two different revolutions, (a) 4,000rpm and (b) 6,000rpm.

As expected the higher revolution provides a bigger RSe improvement (Δq_{geo}), however, no trend within the results is visible. For example, the Silt material changed its behaviour between the condensation regimes. When the Silt material has its lowest adhesion, high (Δq_{geo}) at DRY–series, it is quiet opposite to the other two condensation conditions. However, from observation, higher revolutions (6,000rpm) provide clearer results compared to lower revolutions.

Removal Force Analysis

A second analysis plotted all results versus the resuspension criteria (Eqn. 5-5) of each condensation condition (DRY, REAL and REFERENCE). Image process software (ImageJ) was used to determine the equivalent particle diameter (vertical projection, Submission two), which were used (in classes of 5μm) to calculate the adhesion force and plotted versus $\Delta q_{geo,}$ in Fig. 32(a, b, c).

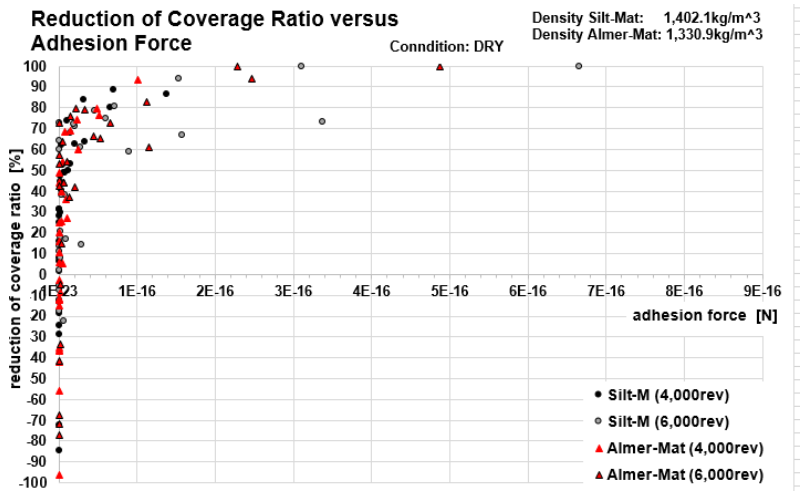

(a)

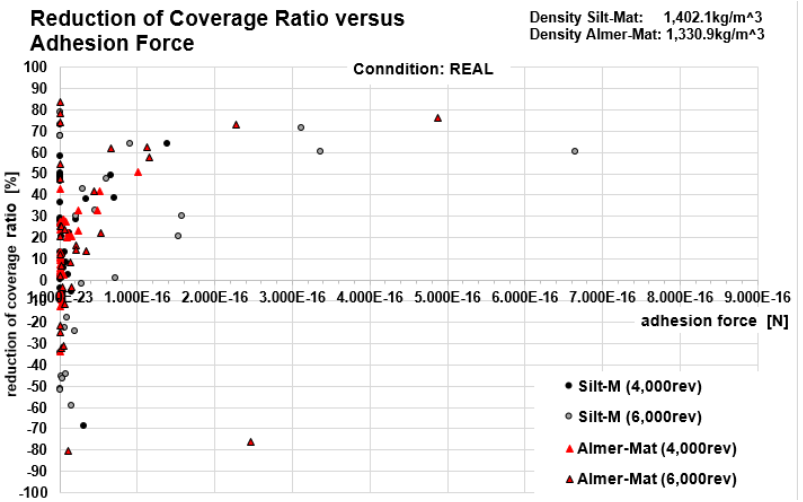

(b)

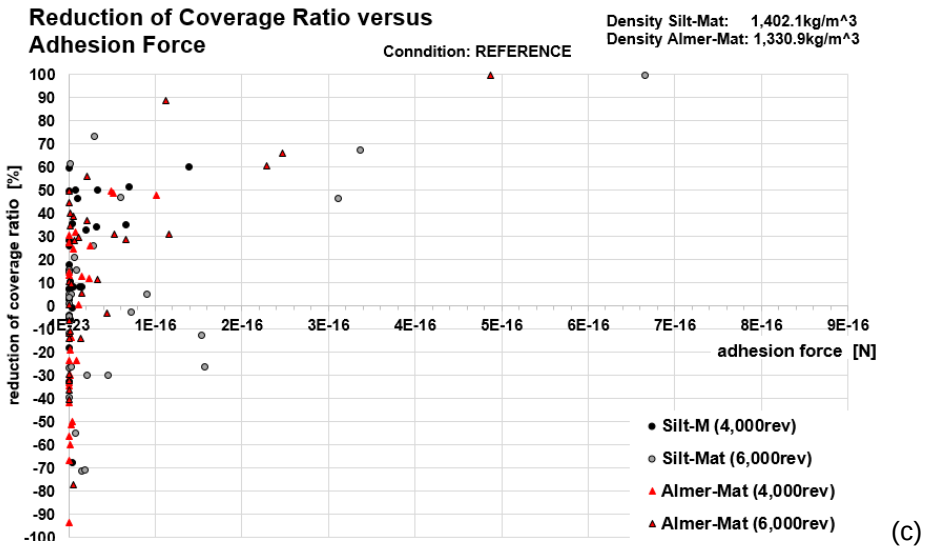

Fig. 32: Three graphs of the condensation experiments, presented as (a) condition DRY, (b) condition REAL and (c) condition REFERENCE.

All cases of results show negative values for the difference in coverage ratio (Δq_{geo}, y axes), which expresses an increase of certain particles, and differences in size and density. This can be observed on the lower end of the adhesion force axis, which is related to smaller particle sizes. This effect is explained in [76], which reports that larger particles have the tendency to resuspend and deposit on the sample surface. This has the effect of particle breaking into smaller particles.

In addition to breakages, smaller particles originally located under bigger particles (particle caking) become visible when observing under SEM and creating microimages.

6 Discussion

6.1 Soiling Process Replication

The developed artificial soiling concept uses a dry method to release the soiling material, a method that guarantee no interference with the previously deposited soiling material already located on the mirror surface. The drop tube design provided excellent and robust results.

The artificial soiling test rig can provide a target soiling load (mass deposition density) to an error of ~16% of target MDD and is consistent. If required, this proportional error can be minimized by adapting the soiling material mass. It was recognized that the remaining error of the soiling load has no or negligible impact in the experimental results and work. The artificial soiling test rig has the capability of repeatable soiling which allowed soiling to a required load. It must be stated that the soiling process must be conducted very carefully in order not to disturb the soiling load already located on a sample.

A further criterion is the equally distributed soiling material on the sample surface. This requirement makes further analysis of the soiled samples possible. The five measurements of RSe on each mirror sample have a tolerance of uniform deposition distribution of +/- 0.04[1] at low MDD, when reducing the soiling area (diameter 32mm) such a distribution can be achieved at a higher MDD too. The threshold is at a MDD value of 1g/m^2. The experimental procedure always averaged the five RSe measurements of one mirror sample and therefore reduced the influence of deposition distribution. In addition, a soiling load below a certain level (< 0.25g/m^2) cannot be distributed equally in a predictable and robust manner. The soiling material is distributed too fast, without any influence of the reduced sieve rotation or reduced oscillation of the device. The influence of the relative humidity (rH) in the lab also has an effect on the release of particles. Up to rH 55% a slow and constant release is possible, beyond this agglomeration and adhesion on the sieve edge makes a robust process impossible. Arizona Test material, originally planned as one of the soiling material, provided similar issues as high rH. After several trials with this material, it was removed from the soiling material list.

Other systems (see below) have a better distribution quality. The reduced soiling area (to improve distribution) is a compromise between method precision (where a large area is required), distribution (where a small area is advantageous) and

the consistency of the location of the five measurements. In addition, it was observed that a soiling load below MDD: 0.25g/m^2 cannot be distributed in a predictable and robust manner.

Sequential soiling was also carried out with target MDD increments of MDD = 0.25g/m^2 and up to 10repeats. The relatively high daily soiling load is required to guarantee a robust and equal particle distribution. As expected, the test series could be processed without any interference on the previous processed soiling material already existing on the sample surface. The end reflectance of the test series has a maximum error to the one off soiling of 6.1% (0.04[1]). This difference highlight the interactions of different effects on the soiling process, however it is assumed that operator handling has the biggest influence. Despite these observations, the “test rig” proved to have the capability to operate single and multiple soiling processes, and therefore is deemed to be a suitable “test rig” for the experimental work for this project.

6.2 Different Artificial Soiling Test Rig Concept

During the international placement in Plataforma Solar de Almeria (Spain), Submission seven, a different artificial soiling test rig was available to test. The “test rig” operates with a dust dispenser, (Solid Aerosol Generator, TOBAS, SAG 410), [78]. The dust dispenser works with a constant airflow, in which the particles are integrated (venture valve). Eight mirror samples are placed in a climate chamber under the airflow, which is directed to the ceiling of the chamber for better distribution. The particle release is controlled by process duration, airflow pressure and two further parameter of soiling material transport. Figure 33 provides an impression of the artificial soiling test rig tested.

(a) (b)

Photo displayed with permission from CIEMAT PSA, Spain.

Fig. 33: Artificial soiling test rig (System CIEMAT/DLR), (a) dust dispenser TOPAS, Solid Aerosol Generator and (b) mirror samples in the soiling chamber. Source: author

The extended trials with Silt material and constant process parameter, revealed the lack of precision of target soiling. An error of up to 112% of soiling load (MDD) between four mirror samples soiled during one soiling process highlights the disadvantage of this system. A further experiment which used exactly the same mirror position twice, also provides differences in soiling load, up to 170% from the target MDD.

From the results of Submission three it is assumed that the airflow and therefore the particle release into the climate chamber is unstable, not constant and unpredictable. Even by keeping the soiling condition, location of mirror sample and process parameter (dust feeding rate), constant the outcome of the soiling load is not consistent.

The average weighted specular reflectance of five locations on the mirror samples were also measured and the standard deviation calculated. The results are better than those from the Cranfield University's soiling test rig. Between 0.01 and 0.25[1] dependent on soiling load, could be analysed, which is 50% of that obtained on Cranfield University's soiling test rig.

6.3 Future Artificial Soiling Test Rig Concept

It is understood, that soiling concepts which provide the soiling material due to airflow provide a much better soiling material distribution, which is lacking on the Cranfield University's soiling test rig. The interference of capillary condensation on the sieve component when releasing the particles will always provide an incoherence in distribution. The reduced capability of sieves to handle larger particle size distribution is an intrinsic flaw. Therefore, the introduction of airflow distribution is the right approach [78, 75], Submission three and seven]. However, target soiling and repeatable soiling under a variety of ambient conditions is a requirement for a future artificial soiling test rig design. It is proposed, that the introduction of several design and process features have the potential to overcome the disadvantages of airflow method.

Recommended features of a future artificial soiling test rig and their advantages:

- The soiling material is distributed with a dust dispenser.

- A large inlet opening compared to the airflow. The stream velocity becomes almost 0m/s which cannot interfere with features within the climate chamber.

- The airflow is constantly active during a soiling session. A stable material transport is guaranteed. The released soiling material can be reused.

- The mirror (glass) sample is located under the climate chamber, separated by an airlock, a shatter which can be open and closed from the outside of the climate chamber.

- The soiling load process is controlled by the opening time of the shutter.

- The soiling load is instantly (quasi full-loop control) measured by locating the sample on a laboratory balance under the climate chamber.

- After a consolidation period of the lab balance, further deposition runs can be carried out, when necessary. A batch process is required.

The combination of airflow method, constant soiling material release and the quasi full-loop controlling of the soiling load could provide an artificial soiling test rig which combines the advantages of the analysed test rigs. Therefore, soiling to target, equal particle distribution and sequential soiling without influencing

effects are provided. Furthermore, humidifier and heating in the lower compartment (lab balance) and different tilt angle can be integrated to simulate different ambient condition.

6.4 Basic Reflectance Model

Soiling Load versus specular Reflectance

Extended soiling experiments with two soiling materials highlighted experimentally the real relationship between both effects. During the sedimentation of particles on the mirror surface, assumed in a randomly manner, two effects are gradually immerging, the shift from primary blocking to secondary blocking and overlapping of particles by settling on each other. The first effect must be taken into consideration when simulating the soiling process, in particular, at very low soiling load, this is the situation when secondary blocking is dominant. High soiling load also has a high geometrical coverage ratio which prevents secondary blocking by the low fraction of uncovered mirror area. The second effect of particle sedimentation is overlapping, which builds up gradually. Further particle sedimentation does not interfere with reflectance, however it increases the mass deposition density. This circumstance can be seen in the empirical model between both parameters. From literature, known linear model (Submission four) becomes an exponential model (assumed in the literature), which fits better, in particular at relative higher soiling load. This was recognized due to experiments with a relatively high soiling load (MDD > 8g/m^2) and numerical analysis. This means that the traditional linear model predicts lower specular reflectance at a specific soiling load. In practical terms, this leads to a reduced number of cleaning cycles being necessary in a given period. Furthermore, the exponential coefficient (C_{MDD}), created by the correlation, represents a specific soiling process, including soiling material characteristic and process characteristic and is therefore potentially a useful parameter to analyse and classify different locations of their soiling reflectance characteristic.

An empirical model of the specular reflectance, based on of the exponential model combining both soiling load effects (mass deposition density and both coverage ratio parameters) was created. This model includes mineral particle specific parameters, such as average particle size ($D_{[4,3]}$) and particle density. The particle volume dependent expression of equivalent particle - diameter (De Brouckere Diameter, $D_{[4,3]}$) was chosen due to its direct connection with particle volume rather than particle area. Furthermore, particle density parameter is the second parameter integrated. The project used a method of extrapolation of a small number (<12measurements) of measurements. This empirical model of

the specular reflectance on the dependency of soiling load and particle characteristic provides the opportunity to model to expect reflectance on the basis of soiling load (solar model operation) and particle parameter (solar field evaluation). It is expected that this model can be expanded and optimized by the integration of further parameters, such as particle shape, mechanical properties of particles, mirror characteristic) and more precise values of input parameter (particle density).

Empirical Soiling Load versus specular Reflectance Model

The overestimation of the reflectance losses by the linear approach compared to the exponential model is soiling load and soiling material dependent. The discrepancy leads to a reduction of cleaning effort. In the case of an assumed specular reflectance of 0.9[1] reduction between15-22% were observed and in the case of RSe 0.8[1] a reduction of 15–25%. A saving of (global) cleaning costs can be assumed conservatively of > 0.5 x 10^6EURO/a.

6.5 Adhesion Effect Experiments

The project analysed adhesion effects of natural soiling, which includes repeatable soiling and in between condensation events. It is assumed that only the replication of the exact process can provide useful results. The results of three test series (DRY, REAL and REFERENCE), with different experimental situation highlighted the differences in the soiling regime.

The project worked with bulk material and averaged material properties rather than material properties distribution. However, it is assumed that future investigations need to integrate the parameter distribution of particles.

Several methods to apply the removal force for the adhesion test were considered. The chosen centrifuge proved to be a practical and effective solution (for horizontal and vertical direction). The limitation of revolutions can be overcome by using a mechanical sample fixture. The removal force is gradually applied, therefore sample damage is avoided. The rig tests bulk material rather than single particles which represents a more natural soiling.

The measurement of the surface free energy of both particles and mirror surface and calculation of the adhesion energy could not be tested due to difficulties in

sample preparation. However, it is assumed, when those difficulties are overcome with a practical method of soiling material preparation, this method should be assessed again.

6.5.1 DRY series

The relatively low adhesion effect due to the absence of condensation and, therefore all the associated effects highlights the need to simulate the condensation phase as well. The outcome differs tremendously with those when condensation was included. The simulation of Van der Waals forces (dry condition) only produces much too low adhesion forces when comparing with adhesion forces which included condensation sequences (natural soiling). Note the project used the DRY series for comparison reasons.

6.5.2 REAL versus REFERENCE series

The main difference between these test series was the soiling (and condensation) regime. Whether, a one-off soiling sequence compared to repeated incremental soiling process must be used in simulating the soiling process. The retrieved results are not consistent which means a general trend is not visible. However, in all groups of results there is a distinguishable difference between both test series. When assuming that the experimental set up and the experimental handling are responsible for these results, so it can be stated that within a test session the results are generated by exactly the same test conditions and therefore present a relative result. There is always a visible different of the results between both test series which highlights the necessary of simulating the soiling process as close as possible to the natural soiling process, otherwise the results are different.

As mentioned earlier, it is assumed that the used experimental test rigs (dry chamber, cooling plate and centrifuge) and the associated test methods must be assessed and where required optimized. The condensation phase has to be more closely controlled and this includes ambient temperature, ambient relative humidity. The cooling plate worked acceptably well; the required temperature was provided. The centrifuge needs improvement, higher revolutions (> 4,000rpm) is required and therefore the used vacuum pad is no longer adequate for sample holding. A mechanical sample fitting is highly recommended. Finally, these results and observation confirm the requirement of using and developing an artificial soiling test rig, which is able to provide sequential soiling.

7 Future Work

During the project, it became obvious that additional components of the soiling process and associated effects must be investigated and therefore to complete the total soiling process, with a soiling model in a holistic way. This includes pre sedimentation situation, the sedimentation process, post-sedimentation, cleaning technology including cleaning strategies and the financial aspects or costs.

The introduction of a consulting service, which provides comprehensive assessments of a proposed solar field in terms of to expect regarding cleaning cost, was not explored during the project. It is also assumed that the aspect of mitigation of aerosol sedimentation needs to be included, too. The reduction of the soiling load on the solar collectors is as important as mitigation of maintenance effort, self-cleaning process' and dust fences are examples.

Furthermore, the post sedimentation effects such as particle caking, capillary aging, cementation and mirror surface degradation belong in a holistic soiling model. The condensation effect on bulk material (and therefore on reflectance), is an issue that is not totally understood. Finally, the long-term effects in soiling, reflectance degradation (due to soiling and cleaning) and the cost implication have to be included in a consultation process. The integration of investigating solar field candidates, or existing solar field operations on optimisation concepts is a missing component in optimizing solar energy industry for the future.

8 Conclusion

Research work in the soiling effect of concentrating solar power requires the replication of the natural soiling process, which includes repeatable soiling and the condensation effect of the soiling process. Therefore, three objectives were stated as follows:

- Design of an artificial soiling test rig
- Gain a better understanding of the soiling process and
- Measurement of adhesion forces between deposited mineral and solar mirror

An artificial soiling test rig was designed and commissioned, to simulate the natural mineral deposition process suitable for research of solar soiling and the mitigation of its negative effects. The test rig enables a defined soiling load to be deposited on to a circular area of a solar mirror specimen. Furthermore the soiling material is equally distributed and therefore suitable for further experiments and measurements.

However, most importantly, the test rig and the experimental method allows for multiple soiling events, so that the soiling material of previous soiling is not compromised.

The artificial soiling test rig works with gravitation and provides a repeatable, robust and precise results (mass deposition density). The constant proportional error of soiling load of 16% was predictable and when required compensated. However, the particle distribution made it necessary to average the measured specular reflectance values.

The project proposes a set of design features for a future artificial soiling test rig design, which will improve future research. The use of an airflow concept to supply the soiling material within a climate chamber proves to have advantages for particle distribution, when soiling to a predicted soiling load (target soiling) is not possible. It is assumed that such a concept in connection with a quasi full loop soiling load control, has the potential to combine the advantages of both designs.

Extended experiments with two soiling material grades with the soiling test rig provided results to formulate an exponential soiling versus reflectance model, a mathematical model, which describes the reflectance of a solar mirror after mineral deposition. At the last stage, the model was extended that mineral properties could be integrated in the model.

The soiling mechanism is governed by primary and secondary blocking and therefore the coverage of the mirror surface by particles has two effects, the geometrical coverage and the effective coverage.

The initial secondary blocking (at low soiling load) is changing to primary blocking with increasing soiling load.

The reflectance versus soiling load must be expressed with an exponential mathematical model. The traditional linear model has an error up to 25% at relatively high specular reflectance (< 0.9[1]).

A specular reflectance model, based on an exponential correlation was created, which integrated parameter of soiling load, average particle diameter and particle density data. This allows prediction based on constituent data rather generalized empirical models. The integration of further parameters (e.g. soiling material properties) could improve the specular reflectance model (particle shape).

The project uses $D_{[4,3]}$ value for particle size and particle density, rather than material density. Both parameters presents the required effects closer to reality.

Finally, even the last WP did not result in a test method to measure the adhesion effect simulation so it highlighted the relevance of the multiple soiling process and condensation phases, which does replicates natural mineral deposition process. The test series, were not conclusive but they highlight the tendency which assumed that repeated soiling and condensation is required.

The centrifuge is a practical and robust test equipment for simulating the removal force. However, the applied 4,000rpm is too low, and as recommended 6,000rpm

or more are required. Furthermore, a mechanical sample fixture needs to be used too.

The final statement of the presented method for analysing adhesion force, a valuable method requires optimisation of the experimental method and equipment would improve the result which includes the controlling of the parameter during condensation, revolution of centrifuge.

References

[1] UN, World Commission on Environment and Development (1987):*"Our Common Future":* https://sustainabledevelopment.un.org/milestones/wced, (accessed 2019)

[2] Harris, J. M., (2000):"*Basic Principles of Sustainable Development":* University Tufts G-DAE, Working Paper No. 00-04, https://sites.tufts.edu/gdae/, (accessed 2020)

[3] Ogunmodimu, O., Okoroigwe, C., (2019):"*Solar thermal electricity in Nigeria: Prospects and challenges"*: Energy Policy 128 (2019), Elsevier Science Ltd., doi.org/10.1016/j.enpol.2019.01.013

[4] Steckel, J., Brecha, R., Jakob, M., Strefler, J., Luderer, G., (2013):"*Assessing future scenarios of energy consumption in developing countries*", Physics Faculty Publications, 18, Ecommons.udayton.edu/phy_fac_pub/18, (accessed 2022)

[5] Akinyele, D., Babatunde, O., Monyei, C., Olatomiwa, L., Okediji, A., Ighravwe, D., Abiodun, O., Onasanya, M., Temikotan, K., (2019):"*Possibilities of solar thermal power generation technologies in Nigeria: Challenge and policy directions*", University Lagos, Nigeria, Renewable Energy Focus, Vol 29

[6] Stocker, T., Platter, G., Qin, D., Tignor, M., Allen, S., Boschung, J., Nauels, A., Xia, Y., Bex, V., Midgley, P., (2013):" *Climate Change 2013: The Physical basics, Summary for Policymakers*", Contribution of working Group I, Cambridge University Press, Cambridge UK and New York USA

[7] Department for Business, Energy and Industrial Strategy, (2020):"*UK Energy in Brief 2019*"

[8] Chen, K., Winter, R., Bergman, M., (1980):"*Carbon dioxide from fossil fuels*", University Michigan, Energy Policy, IPC Business Press, 0301-4215/80/040318-13

[9] International Energy Agency, (2022):"*CO2 Emissions in 2022*", IEA Paris, F, from www.iea.org, (assessed 2023)

[10] BP (2022):"*Energy Outlook 2022*", BP energy economics, BP plc 2022, from: bp.com/content/dam/bp/business-sites/en/global/corporate/pdfs/energy-economics/energy-outlook/bp-energy-outlook-2022.pdf, (assess 2023)

[11] D Statis, "*Energy consumption of private households*", Statistische Bundesamt, Wiesbaden, D, available: https://www.destatis.de/EN/Service/Contact/_Contact.html (accessed: 2020)

[12] Eurostat, "*Energy consumption in households*", Eurostat, Statistics explained, Luxembourg, available: https://ec.europa.eu/eurostat/statistics-explained/index.php?title=Energy_consumption_in_households, (accessed: 2023)

[13] Kumar, V., Shrivastava, R., Untawale, S., (2015):"*Solar Energy: Review of Potential Green & Clean Energy for Coastal and Offshore Applications*", International Conference on Water Resources, Coastal and Ocean Engineering 2015, Aquatic Prodedia 4 (2015), ELSEVIER

[14] Mauthner, F., Weiss, W., Spoerk-Duer, M., (2014):"*Solar Heat Worldwide 2016*", Solar Heating & Cooling Programme, International Energy Agency, Paris F

[15] IRENA, (2012):"*Concentrating Solar Power*", Renewable energy technology: cost analysis series, Vol 1 Power Sector, International Renewable Energy Agency, Abu Dhabi, UAE

[16] IRENA, (2018):"*A Roadmap to 2050*", Global Energy Transformation, International Renewable Energy Agency, Abu Dhabi, UAE, ISBN 978-92-9260-059-4

[17] Goswami, D., (2015):"*Principles of Solar Energy*", CRC Press, Taylor & Francis Group LLC, ISBN 13: 978-1-4665-6379-7, Boca Raton FL, USA

[18] Soomo, M., Mengal, A., Memon, Y., Khan, M., Shafiq, Q., Mirjat, N., (2019):"*Performance and Economic Analysis of Concentrated Solar Power Generation for Pakistan*", processes 2019, MDPI, mdpl.com/journal/energies, doi: 10.3390/pr7090575

[19] Stine, W., Geyer, M., "*Solar Energy System Design", in Power from the Sun*, (California State Polytechnic University, Pomona, USA, 1993, available at: http://www.powerfromthesun.net, (accessed 2021)

[20] Trieb, F., (2005):"*Concentrated Solar Power for the Mediterranean Region, final report*", German Aerospace Centre (DLR), from: www.dlr.de/tt/med-csp

[21] Knies, G., (2007):"*Cleaner Power from the Deserts, White Book 4th edition*", Desertec, Hamburg, Protex Verlag Bonn, ISBN 978-3-929118-67-4

[22] Trieb, F., Schilling, O'Sullivan, M., Pregger, T., Hoyer-Klick, C., (2009):"*Global Potential of Concentration Solar* Power", German Aerospace Centre, Stuttgart, D, SolarPaces Confernece Berlin

[23] Kurup, P., Turchi, C., (2015):"*Initial investigation into the potential of CSP industrial process heat for the USA*", NREL, Denver USA, NREL/TP-6A20-64709, www.osti.gov/scitech

[24] Champerlain, K., (2019):"*CSP tech leaps set to cut reflector losses, water costs*", https://analysis.newenergyupdate.com/csp-today/csp-tech-leaps-set-cut-reflector-losses-water-costs, (accessed 2022)

[25] Scheer H., (1995):*"Solar energy's economic and social benefits",* Solar Energy Materials and Solar Cells 38, p555-568, Elsevier Science Ltd.

[26] Hewitt, G., Shires, G., Polezhaev, Y., (1997):"*Inter. Encyclopaedia of Heat & Mass Transfer*", CRC Press LLC, Florida, USA, ISBN 0-8493-9356-6

[27] Duffie, J., Beckman, W., (2013):"*Solar Engineering of Thermal Processes*", Fourth Edition, published by John Wiley & Sons, Inc., USA, ISBN 978-0-470-87366-3

[28] Mertens, M. (2009):"*Technische und wirtschaftliche Analyse von horizontalen Fresnel-Kollectoren*", Fakultaet fuer Maschinenbau, Universitaet Karlsruhe, Thesis

[29] IEA, (2010):"*Technology Roadmap Concentration Solar Power*", International Energy Agency, Paris, F

[30] Ilse, K., Figgis, B., Naumann, V., Hagendorf, C., Bagdahn, J., (2018):"*Fundamentals of soiling processes on photovoltaic modules*", Renewable and sustainable energy reviews 98

[31] Roth, P., Pettit, R., (1980):"*Effect of soiling on solar mirrors and techniques used to maintain high reflectivity*", ResearchGate, doi:10.1016/b978-0-12-511160-7.50013-2, www.researchgate.net/publication/236554434

[32] Schill, C., Anderson, A., Baldus-Jeursen, C., Burnham, L., Micheli, L., Parlevliet, D., Pilat, E., Stridh, B., Urrejola. E., (2022):"*Soiling losses – impact on the performance of Photovoltaic power plants",* IEA PVPS Task 13, performance, operation and reliability of PV systems, ISBN 978-3-907281-09-3

[33] Ilse K., Micheli L., Figgis B. W., Lange K., Dassler D., Hanfi H., Wolferstetter F., Naumann V., Hagendorf C., Gottschalg R., Bagdahn J., (2019):"*Techno-Economic Assessment of soiling losses and mitigation strategies for Solar Power Generation*", Joule, 3, 2303, Elsevier. CellPress

[34] Sayyah, A., Horenstein, M. Mazumder, M., (2014):"*Energy yield loss caused by dust deposition on PV panels*", University Boston, USA, ResearchGate, doi:10.1016/j.solener.2014.05.030, www.researchgate.net/publication/266258869

[35] Branke, R., "*CSP Plant Operations & Maintenance"*, ISE Fraunhofer Institute, 2nd MENA CSP KIP Workshop, Feb. 2018, Hyatt Regency Creek Heights, Dubai

[36] Ba, H., Chlette, M., Wang, R., Borghesani, P., Ma, L., Steinberg, T., (2017):"*Optimal condition-based cleaning of solar power collectors"*, Solar Energy 157 (2017) 762-777, Elsevier ltd

[37] Sharma, D., Ali, A., Sharma, D., (2021):"*A mini review on the effect of cleaning strategies on productivity of various solar thermal collectors*", International Conference on Futuristic Technologies Jan 2021, paper no FT-21054, www. Researchgate.net/publication/348803582

[38] Solar Millenium, "*Andasol–the world's largest solar thermal power plant project development in Andalucia (Spain*)", Solar Millenium, Erlangen G, www. Solar Millenium.de

[39] IRENA (2020):"*RE-Capacity Statistics*", International Renewable energy agency, Masdar City UAE, www.irena.org/Publications (accessed 2021)

[40] Brophy, B., Pop, S., Schulze, R., Yang, S., Maghsodi, S., Gonsalves, P.*: "Highly Durable Anti-Reflective Anti-Soiling Coating for PV Module Glass",* Presentation Poster, Yingli Green Energy Americas, Enki Technology, CA USA

[41] Wette, J., Fernandez-Garcia, A., Sutter, F., Buendia-Martinez, F., Arguelles-Arizeun, D., Azpitarte, I., Perez, G., (2019):"*Water Saving in CSP Plants by a Novel Hydrophilic Anti-Soiling Coating for Solar Reflectors*", MPDI Coatings 2019,9,739; doi:10.3390/coatings9110739

[42] Bennett, A., Sansom, C., King, P., Gobey, C., Merkle, H., (2019):"*Cleaning Concentrating Solar Power Mirror without Water*", SolarPACES 2019, AIP Conf. Proc. 2303, 210001, 2020

[43] PVRadar: "*World-class performance and reliability*", Company web site, PVRADAR labs GmbH, Bay, De, www.pvradar.com, (accessed 2023)

[44] Solar Unsoiled: "*Maximize solar PV performance, reclaim lost profit*", Company web site, Solar Unsoiled, NC USA, www.solarunsoiled.com, (accessed 2023)

[45] Adak, D., Bhattacharyya, R., Barshilia, H., (2022):"*A state of art review on the multifunctional self-cleaning nanostructured coatings for PV panels, CSP mirrors and related solar devices*", Renewable and Sustainable Energy Reviews 159 (2022) 112145, doi.org/10.1016/j.rser.2022.112145

[46] IEA PVPS Task 13, (2022):"*Soiling Losses-Impact on the Performance of Photovoltaic Power Plants*", International Energy Agency, Performance, Operation and Reliability of PV Systems, Report IEA-PVPS T13-21:2022, ISBN 978-3-907281-09-3

[47] Covesto, “Anti Soiling coating for solar glass”, product information, Covesto Deutschland AG, Leverkussen D, web site: www.covestro.com, (accessed 2024)

[48] Sansom, C., Patchigolla, K., (2017):“*Water Management Guide”*, Deliverable: D4.2, H2020-LCE-02-2015, (WASCOP project, Water Saving for Solar Concentration Power

[49] Kaldellis, J., Fragos, P., Kapsali, M., (2011):”*Systematic experimental study of pollution deposition impact on the energy yield of photovoltaic installations”*, Renewable Energy 36, Elsevier Science Ltd., 2011

[50] Burton, P., King, B., (2013):”*Artificial Soiling of Photovoltaic Module Surface using Traceable Soil Components”,* Sandia National Laboratories Albuquerque NM 87185 USA, 978-1-4799-3299-3/13 IEEE, 2013)

[51] Boppana, S., Rajasekar, V., Samy, G., Mani, T., (2016):”*Working towards the development of a Standardized Artificial Soiling Method”,* Thesis, Arizona State University PV Reliability Laboratory, Arizona, USA

[52] Burton, P., King, B., (2014):”*A Handbook on Artificial Soils for Indoor PV Soiling Tests”,* Sandia National Laboratories Albuquerque NM 87185 USA, SAND2014-19199

[53] Klimm, E., Ost, L., Koehl, M., Weiss, K., (2016):”*Microscopic measurement and analysis of the soiling behaviour of surfaces with standardized and real dust–a parameter study*“, Energy Procedia 91 (2016), Elsevier Ltd., presented SHC 2015

[54] Mantha, S., (2016):”*Development of Uniform Artificial Soil Deposition Techniques on Glass and PV Coupons”,* Thesis, Arizona State University, Arizona, USA

[55] Klimm, E., Lorenz, T., Weiss, K., (2013):”*Can anti-soiling coating on solar glass influence the degree of performance loss time of PV modules drastically?* (28th European PV solar energy conference”, 2013, Paris, F

[56] Wolferstetter, F., Sansom, C., King, P., Wilbert, S., Fernandez Garcia, A., (2018):“*Soiling and condensation model applied to CSP solar field”*, Deliverable: D3.2, H2020-LCE-02-2015, (WASCOP project, Water Saving for Solar Concentration Power, Sponsor: European, 2018.

[57] Ilse, K., Zahid Khan, M., Lange, K., Gurumoorthy, H., Naumann, V., Hagendorf, C., Baghan, J., (2020):*“Rotational force test method for determination of particle adhesion–from a simplified model to realistic dusts*“, Journal of renewable and sustainable energy 12 043503 (2020), doi.org/10.1063/10.1063/5.0015122

[58] **Aragon Photonics, "*Solar Instruments*",** Aragon Photonics Labs. S.L.U., Zaragoza, Spain, www.aragophotonics.com, (accessed 2020)

[59] International Standard, (1992):"*Solar energy–reference solar spectral irradiance at the ground at different receiving conditions–Part 1 Direct normal and hemispherical solar irradiance for air mass 1.5*", ISO 9845-1: 1992 (E), ISO Geneva, CH

[60] Levitan, D., (2013):"*How do you clean 250 thousand solar thermal mirrors? Trucks with robot arms*!" IEEE Spectrum, available at: spectrum.ieee.org/how-do-you-clean-258048-solar-thermal-mirrors-trucks-with-robot-arms, (accessed 2023)

[61] Health and Safety Executive, (2002):*"Workplace Exposure Limits fourth edition*", Health and Safety Executive, ISBN 978 0 7176 6733 8, fours edition came to force on the 17th Jan 2020.

[62] IMA-Europa, (2020):"*Sichere Umgang mit Quartsfeinstaub*", SafeSilica, IMA-Europa AISBL (NIEPI-Sekretariat) 26. Rue des Deux Eglises, Bruessel, B, available: www.safesilica.eu, (accessed 2020)

[63] Wolfertstetter, F., (2016):"*Auswirkungen von Verschmutzungen auf konzentrierende solarthermische Kraftwerke*", Thesis, Rheinisch-Westfaelischen Technischen Hochschule Aachen, Fakultaet fuer Maschienwesen, DLR Solarforschung

[64] Roth, P., Pettit, R., (1980):*"Effect of soiling on solar mirrors and techniques used to maintain high reflectivity"*, Sandia Lab, Albuquerque NM, USA, ResearchGate, doi10.1016/b978-0-12511160-7-50013-2

[65] Kaldellis, J., Kapsali, M., (2011):"*Simulating the dust effect on the energy performance of PV generators based on experimental measurements*", Energy 36 (2011), 2011 2012 Elsevier Ltd., doi: 10.1016/j.energy2011.06.018

[66] Helmsath, A., Lindner, P., Klimm, E., (2016):"*Specular Reflectance of soiled glass mirrors – study on the impact of incidence angles*", AIP Conference Proceedings 1734, 130009 (2016), doi.org/10.1063/1.4949219

[67] Ilse, K., Zahid Kahn, M., Voicu, N., Naumann, V., Hagendorf, C., Bagdahn, J., (2019):"*Advanced performance testing of anti-soiling coatings-Part I: Sequential laboratory test methodology covering the physics of natural soiling processes*", Solar Energy Materials and Solar Cells 202 (2019) 110048, Elsevier B.V. doi.org/10.1016/j.solmat.2019.110048

[68] Ilse, K., Zahid Khan, M., Lange, K., Gurumoorthy, H., Naumann, V., Hagendorf, C., Baghan, J., (2020): *"Rotational force test method for determination of particle adhesion – from a simplified model to realistic dusts*", Journal of renewable and sustainable energy 12 043503 (2020), doi.org/10.1063/10.1063/5.0015122

[69] Israelachvili, J., (2011):"*Intermolecular and Surface Forces, third edition*", Academic Press, ISBN: 978-0-12-375182-9

[70] Duenisch, S., (2005):"*Untersuchung der Wirkungsweise von Nanomaterialien*", thesis for phd, University Wuerzburg

[71] Masuda. H., Higashitani, K., Yoshida, H., (2006):"*Powder Technology Handbook, third edition*", CRC press, Taylor & Francis Group LLC, USA, ISBN: 1-57444-782-3

[72] Mullins, M., Michaelis, L., Menon, V., Locke, B., Ranade, M., (1992):"*Effect of geometry on particle adhesion", Aerosol Science and technology*, 17:2. doi.org/10.1080/02786829208959564

[73] Zafar, U., Hassanpour, A., Ghadiri, M., (2014):"*Drop Test: A new method to measure the particle adhesion force"*, Powder Technology 264 (2014), Elsevier B.V. doi.org/10.1016/j.powtec.2014.04022

[74] El Baraka, A., Ennaceri, H., Ennaoui, A., Ghennioui, A., Jorio, A., Khaldoun, A., (2019):"*A novel approach to evaluate the soiling adhesion on the surface of CSP reflectors via extended DLVO theory*", Applied Physics A: Materials Science & Processing. Aug2019, Vol. 125 Issue 8, doi: 10.1007/s00339-019-2809-0

[75] Shimada, Y., Tsubota, M., Matsusaka, S., (2022):"*Measurement of particle adhesion force and effective contact radius via centrifuge equipped with horizontal and vertical substrates"*, Powder Technology 397 (2022) 117103, Elsevier B.V. doi.org/10.1016/j.powtec.2021.117103

[76] Ilse, K., Zahid Kahn, M., Voicu, N., Naumann, V., Hagendorf, C., Bagdahn, J., (2019):"*Advanced performance testing of anti-soiling coatings-Part II: particle-size dependent analysing for physical understanding of dust removal processes and determination of adhesion forces*", Solar Energy Materials and Solar Cells 202 (2019) 110049, Elsevier B.V. doi.org/10.1016/j.solmat.2019.110049

[77] Figgis, B., Nouviaire, A., Wubulikasimu, Y., Javed, W., Guo, B., Ait-Mokhtar, A., Belarbi, R., Ahzi, S., Remond, Y., Ennaoui, A., (2018):"*Investigations of factors affecting condensation on soiled PV modules",* Solar Energy, 159 (2018), doi.org/10.1016/j.solener.2017.10.089

[78] TOPAS, "*Staubgenerator, Serie SAG 410*", manual instruction, TOPAS, Dresden, Germany, www.topas-gmbh.de

Appendices

Appendix A Ethical Approval Letter

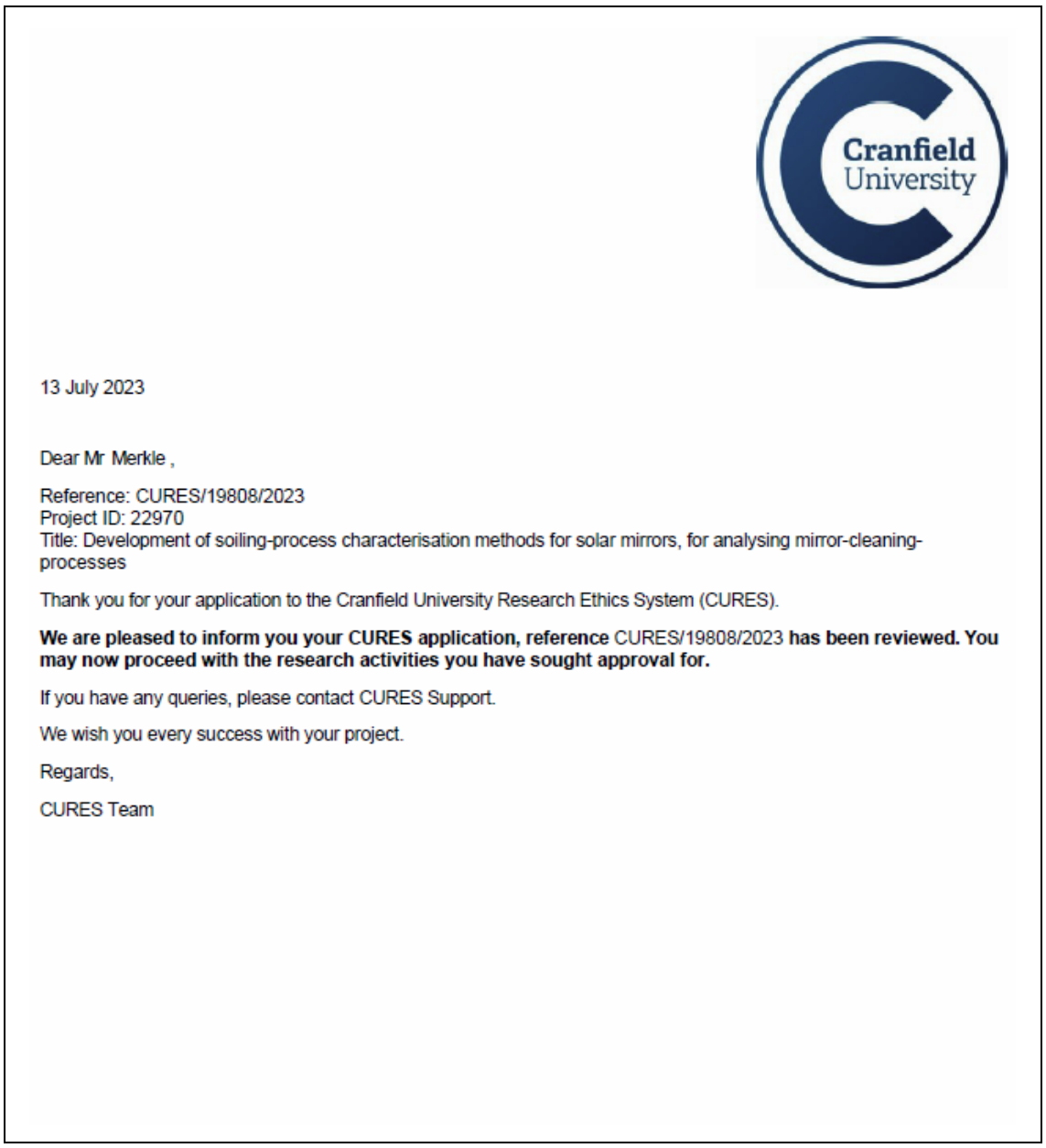

13 July 2023

Dear Mr Merkle ,

Reference: CURES/19808/2023
Project ID: 22970
Title: Development of soiling-process characterisation methods for solar mirrors, for analysing mirror-cleaning-processes

Thank you for your application to the Cranfield University Research Ethics System (CURES).

We are pleased to inform you your CURES application, reference CURES/19808/2023 **has been reviewed. You may now proceed with the research activities you have sought approval for.**

If you have any queries, please contact CURES Support.

We wish you every success with your project.

Regards,

CURES Team

Appendix B Additional Material

B.1 CSP Capacity and Aperture area for the period 2008 to 2026

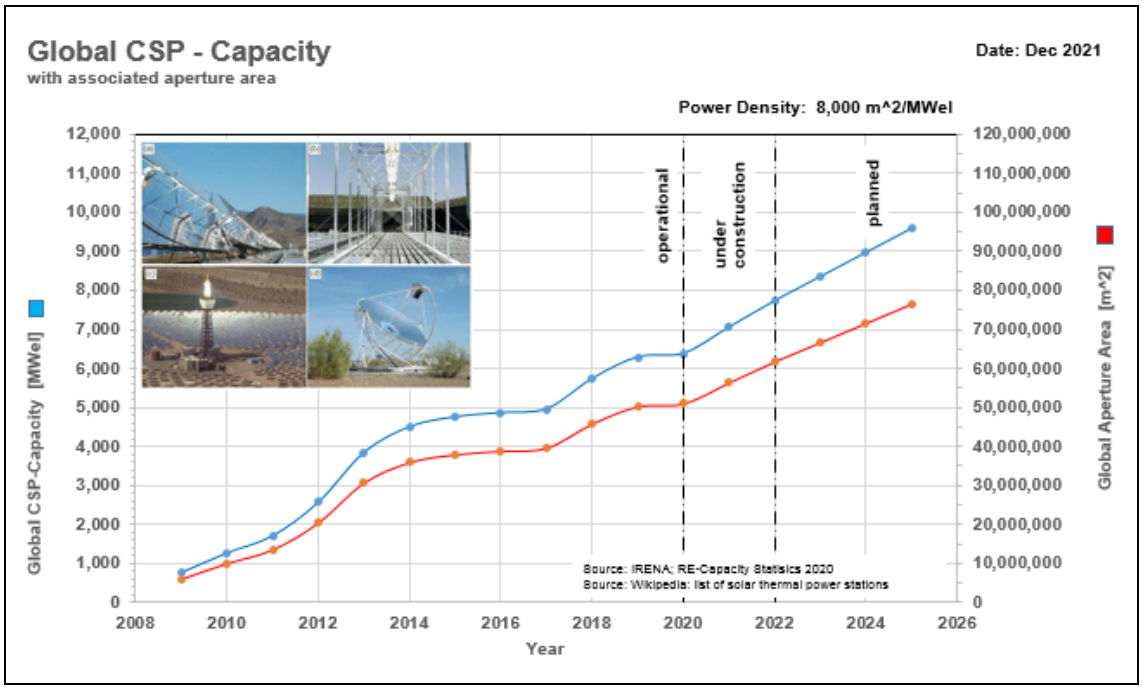

B.2 Images of the Artificial Soiling Test Rig

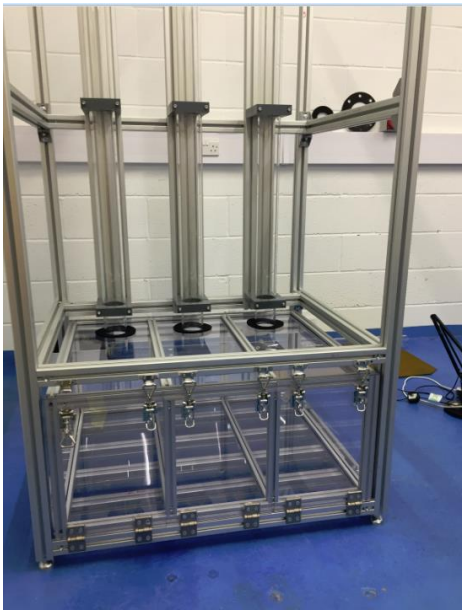

(a)

(b)

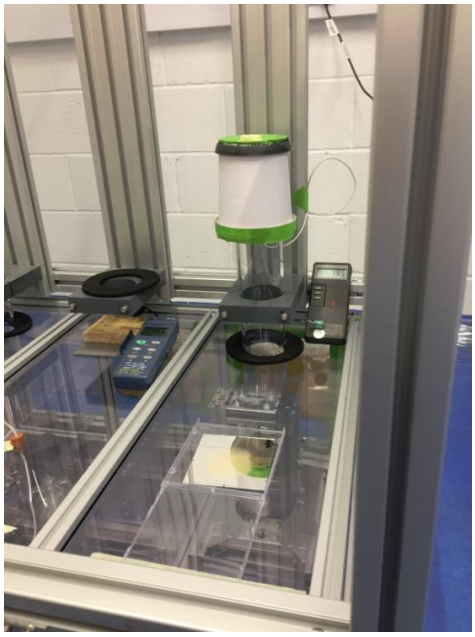

(c)

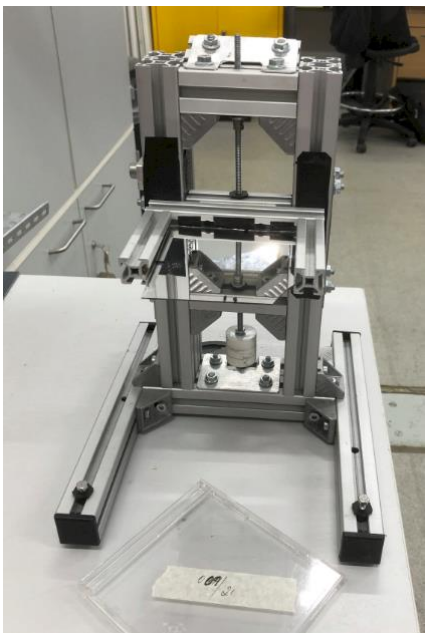

(d)

(a) Image of all three climate chambers of the artificial soiling test rig, (b) view into the right climate chamber visible is the lower opening of the drop pipe, (c) top view of the right climate chamber with the 500mm drop pipe and the rotatable release sieve and (d) the sample frame with mirror sample, located in the climate chamber.